Charging of Elk Hills reservoirs as determined by oil geochemistry

John E. Zumberge, Judy A. Russell, and Stephen A. Reid

AUTHORS

JOHN E. ZUMBERGE ~ *GeoMark Research, Ltd., 9748 Whithorn Drive, Houston, Texas 77095; jzumberge@geomarkresearch.com*

John E. Zumberge has been vice president and cofounder of GeoMark Research in Houston since 1991. He was manager of geochemical and geological research for Cities Service–Occidental, general manager for Ruska Laboratories, and director of geochemical services for Core Laboratories. He has global experience in petroleum geochemistry, focusing on crude-oil biomarkers. He obtained a B.S. degree in chemistry from the University of Michigan and a Ph.D. in organic geochemistry from the University of Arizona.

JUDY A. RUSSELL ~ *Occidental Oil and Gas Corporation, Suite 110, 5 Greenway Plaza, Houston, Texas 77046; judy_russell@oxy.com*

Judy A. Russell is a senior geological advisor for Occidental and works on worldwide exploration and production, with an emphasis on the integration of geochemistry. She has extensive experience in many of Occidental's projects in Latin America, Far East, the United States, and the Middle East. She has a B.S. degree from Phillips University and an M.S. degree from the New Mexico Institute of Mining and Technology.

STEPHEN A. REID ~ *Occidental Oil and Gas Corporation, Suite 110, 5 Greenway Plaza, Houston, Texas 77046; tony_reid@oxy.com*

Stephen Anthony Reid is a senior geological advisor for Occidental and works on international exploration, with an emphasis on deep-water projects. He has extensive experience in California's San Joaquin basin, including the Elk Hills field, where he conducted studies on Stevens turbidite and Monterey porcelanite reservoirs. He has B.S. and M.S. degrees from California State University, Northridge.

ABSTRACT

Crude oils from Miocene and Pliocene reservoirs from the Elk Hills field in California's San Joaquin basin were analyzed for stable carbon isotopes and biomarkers. Cluster analysis of geochemical variables defines five principal oil families, all derived from different organic-rich facies of the Miocene Monterey Formation. Carbon isotope analysis indicates no contribution from the basin's other major source rock, the Eocene Kreyenhagen Formation. Oil families show a strong correspondence to stratigraphic intervals. Oils from pre-Monterey reservoirs were probably generated from the lowermost organic-rich facies of the Monterey and are the most thermally mature. Upper Miocene Stevens zone turbidite reservoirs contain oils of various thermal-maturity stages, but mature light ends are abundant and are likely generated from the floors of the adjacent subbasins located north and south of Elk Hills. The relatively minor presence of low-thermal-maturity biomarkers that are typically characteristic of Monterey oils may indicate that Stevens traps did not form until after the source intervals were at a higher level of thermal maturity. All oils in Stevens porcelanite reservoirs contain a higher concentration of low-maturity biomarkers, which may indicate derivation from more localized areas on the flanks of the Elk Hills anticlines. The shallow Pliocene oils have suffered biodegradation to different degrees, and the lowest API gravities occur on the flanks of the anticline. The carbon isotopic composition of these oils suggests yet another Monterey source facies that charged the Pliocene reservoirs and is not simply the result of vertical leakage from the older Miocene reservoirs.

INTRODUCTION

Oils from California's San Joaquin basin are derived from Eocene and Miocene source intervals (Zieglar and Spotts, 1978; Kruge 1986; Peters et al., 1994; Kaplan, 2000). Expulsion and migration

of oil from the deeper, thermally mature areas of the basin began in the Pliocene and is coincident with the initiation of deformation that forms many of the basin's structural traps. Other than the general relationship of oils to source rocks, little additional information has been published for the basin documenting specifics of expulsion timing, migration pathways, and filling (or charging) of traps. This study presents a detailed look at oils from the Elk Hills field and nearby fields and indicates that oil families differ by reservoir composition, depth, and location. These subtle distinctions reflect a complex expulsion and migration history at Elk Hills and provide clues on the timing of trap formation and the filling sequence of oil reservoirs.

This study presents geochemical data and interpretations for 66 oils from the Elk Hills field, San Joaquin Valley, California. Most of the samples are from turbidite sandstone and porcelanite reservoirs of the upper Miocene Monterey Formation. Pre-Monterey and Pliocene reservoirs are also incorporated. In addition, 10 oils from other southern San Joaquin fields, mostly from pre-Monterey reservoirs, were included for comparison. The purpose of this study is to determine the origin and potential migration pathways for Elk Hills oils, including those produced from the older reservoirs as well as the shallow Pliocene zones. Whether pre-Monterey source units are present in Elk Hills (e.g., Eocene Kreyenhagen or lower Miocene Temblor) is important, considering not only the deep potential in Elk Hills, but also other deep targets in the southern San Joaquin Valley.

Based only on a limited oil sample data set, Peters et al. (1994) distinguished San Joaquin oils derived from the Miocene Monterey and the Eocene Kreyenhagen source rocks using primarily stable carbon isotopic compositions. Typical of marine Miocene-derived oils worldwide, oils derived from the Monterey are isotopically heavy (more positive), whereas the Eocene oils are 4–5‰ lighter (more negative). These petroleum system assignments were confirmed by source rock analyses (Peters et al., 1994). With this limited data set, Peters et al. (1994) determined that Eocene oils are present in the northern San Joaquin basin and extend as far south as the Belgian Anticline field, which is located just to the west and northwest of Elk Hills (Figure 1). Oils in the central and southern San Joaquin basin are derived from Miocene source rocks.

In 1999, the first 15 oils from Elk Hills were analyzed for this study. Two of these oils were from pre-Monterey reservoirs (Temblor Formation) and differed in their biomarker chemistry (molecular fossils) from most of the oils produced from various Stevens sandstone units. The stable carbon isotopic composition of the C_{15+} fractions still indicated a Monterey source for these Temblor oils, at least for the heavy-oil fraction. These first studied Elk Hills oils were also compared to other Monterey oils from the Santa Maria, Santa Barbara Channel, and Los Angeles basins. The lower phosphatic and carbonate-rich facies of the Monterey generated much of the oil found in the Santa Maria and Los Angeles basins (e.g., Isaacs and Rullkötter, 2001), whereas Elk
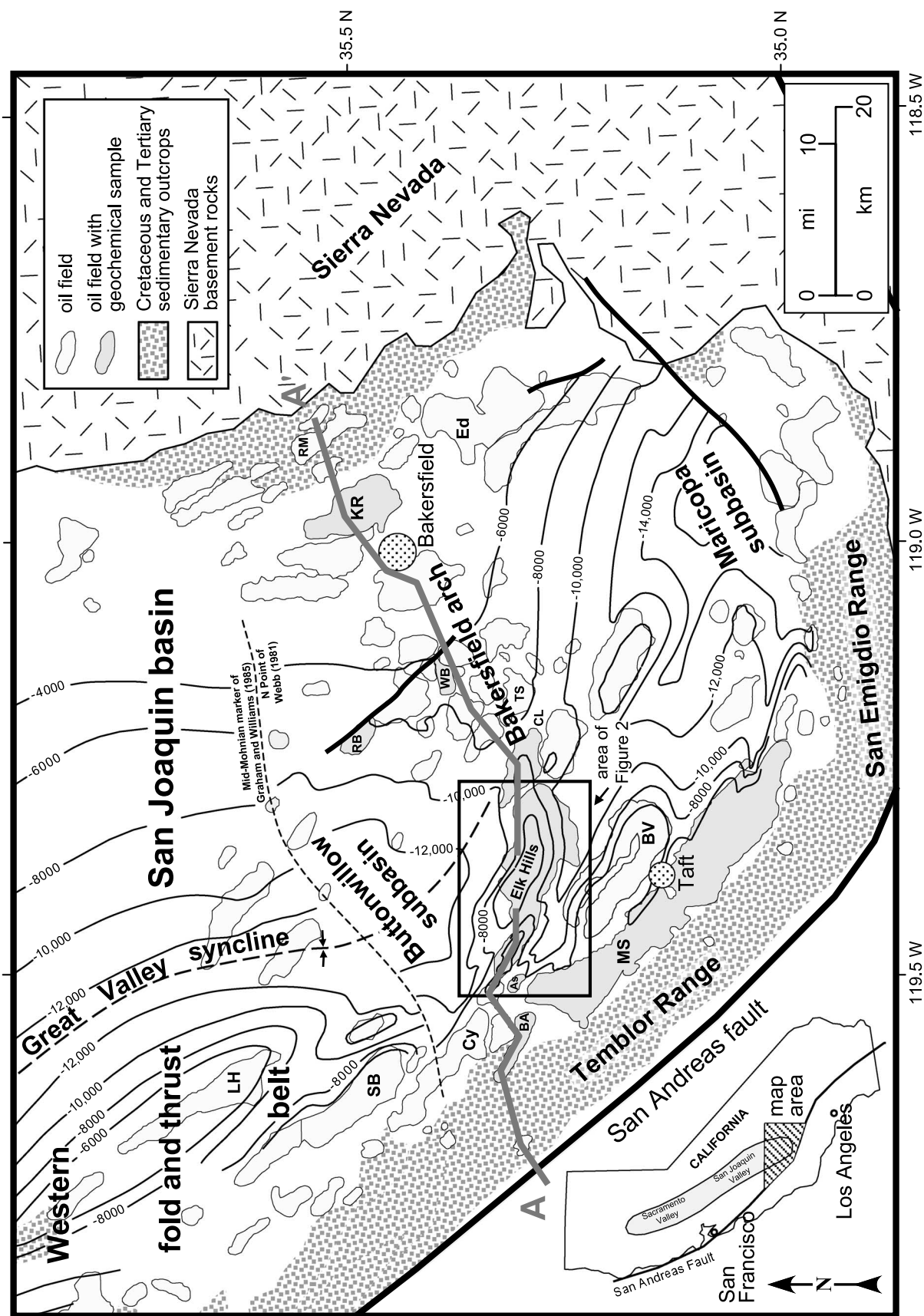
Figure 1. Index map of the southern San Joaquin basin, showing the major structural features and significant oil fields. Simplified structural contours are of Graham and Williams' (1985) mid-Mohnian marker and Webb's (1981) N Point. Key to field names: As = Asphalto; BA = Belgium Antidine; BV = Buena Vista; CL = Coles Levee; Cy = Cymric; Ed = Edison; KR = Kern River; LH = Lost Hills; MS = Midway-Sunset; RB = Rio Bravo; RM = Round Mountain; SB = South Belridge; TS = Ten Section; and WB = West Bellevue.

Hills Monterey oil biomarkers appear to originate primarily from more siliceous Monterey facies based on biomarker distributions. Subsequently, 51 additional Elk Hills oils were analyzed to include additional pre-Monterey reservoirs as well as porcelanite and shallow oil zone samples. Ten oils from other southern San Joaquin fields, including Eocene Kreyenhagen-derived oils, were also analyzed. The pedigrees of all oils are listed in Table 1.

REGIONAL GEOLOGIC SETTING, SOURCE ROCKS, AND RESERVOIRS

Elk Hills is located in the southern San Joaquin basin, about 40 mi (65 km) southwest of Bakersfield, California (Figure 1). The basin is a prolific hydrocarbon region and has produced more than 12 billion bbl oil and 3.5 tcf gas (California Division of Oil, Gas, and Geothermal Resources, 2003). The basin is asymmetrical along a north-south–trending axis (the Great Valley syncline) and is filled with sediments of late Mesozoic and Cenozoic age. On the east side of the basin, the basin fill thins as it onlaps Mesozoic igneous basement and forms a homoclinal limb that is locally broken by Miocene and Pliocene extensional faulting. The stratigraphic section thickens westward and is more than 25,000 ft (7620 m) thick west of the axis. The west side of the basin, which terminates at the San Andreas fault, is strongly deformed because of Pliocene to Holocene compression, and parts of the Cretaceous to Miocene section are exposed in outcrop. Several large anticlines, including Buena Vista, Belridge, and Lost Hills, are part of Bartow's (1991) western fold and thrust belt and formed during this period of compression. A broad northeast-trending basement ridge, the Bakersfield arch, divides the southern San Joaquin basin into the Maricopa and Buttonwillow subbasins. The Elk Hills field lies between the two subbasins southwest and along trend with the arch and merges westward into the western fold and thrust belt.

The principal petroleum source facies of the basin are the middle to upper Eocene Kreyenhagen Formation and the middle and upper Miocene Monterey Formation (Figure 2). The Kreyenhagen Formation is present in the subsurface throughout the Buttonwillow subbasin and extends at least as far south as Elk Hills and the Bakersfield arch. The Kreyenhagen consists of shale and siliceous shale and is up to 1000 ft (305 m) thick in the Buttonwillow subbasin (Church and Krammes, 1957; Villanueva and Kappeler, 1989).

It was deposited under restricted marine conditions when the basin was partially closed along its western margin (T. H. Nilsen, S. A. Reid, D. R. D. Boote, 2005, personal communication). Along the west side of the basin, submarine-fan deposits of the Point of Rocks Sandstone Member are encased within the Kreyenhagen (Nilsen, 1987). Total Kreyenhagen and Point of Rocks thickness west of Elk Hills is about 6500 ft (2000 m) (Dunwoody, 1986) (Figure 3). Organic content is moderate to high (Kaplan, 2000) and consists of marine kerogen. The Kreyenhagen is a good source rock and is the source of oils in most of the fields in the northern Buttonwillow subbasin (Peters et al., 1994; Kaplan, 2000).

The Monterey Formation is present in the subsurface in the central and western areas of the Buttonwillow and Maricopa subbasins as well as across the Bakersfield arch. West of the basin axis and east of the outcrop belt, the formation is more than 5000 ft (1524 m) thick (Graham and Williams, 1985) (Figure 3). A complex lithologic suite is present that includes diatomite, porcelanite, siliceous shale, chert, clay-shale, and dolomite. In the Elk Hills area, the Monterey was deposited in a dynamic setting of evolving subsea structures in a deep-water setting (~2000–4000 ft; ~600–1200 m; Bandy and Arnal, 1969). Deposition of the Monterey occurred after the development of the San Andreas fault and the transformation of the San Joaquin basin from a convergent to a transform margin setting (Graham et al., 1989). By the late Miocene, wrench tectonism caused several San Joaquin structures to begin growing, including those at Buena Vista Hills, Elk Hills, and Lost Hills (Harding, 1976). Based on paleogeographic reconstructions by Graham (1978) and Graham et al. (1989) that include restoration of 165 mi (265 km) of post-Miocene offset on the San Andreas fault, emergent granitic basement of the Salinian block lay west of the basin and resulted in the basin's partial closure. The deep-marine setting became ideal for the preservation of organic-rich diatomaceous source rocks (Graham and Williams, 1985). Organic-rich shales collected in abundance in areas removed from coarse-grained deposition, including on the crests of the growing subsea anticlines. Thick turbidite sandstones, collectively referred to informally as the Stevens sand (and by numerous local names), are derived from highlands on the west, south, and east sides of the basin (MacPherson, 1978; Webb, 1981) and are interbedded within the Monterey, mostly in the upper half of the formation. Organic material from the Monterey Formation is established as the source of oil

in oil fields in the Maricopa and southern Buttonwillow basins (Peters et al., 1994; Kaplan, 2000).

Although the Miocene and Pliocene part of the stratigraphic section in the Elk Hills area and the central San Joaquin basin is composed primarily of mudstone, claystone, and siliceous shale, at five distinct time intervals, depositional systems brought reservoir-quality sands to the basin center (Figures 2, 3): (1) early Miocene western-sourced Santos and Carneros fans; (2) late Miocene eastern-derived Stevens submarine fan; (3) late Miocene western-derived Stevens turbidites; (4) early Pliocene Etchegoin–San Joaquin tidal system; and (5) late Pliocene Mya tidal channels (Reid, 1995).

The oldest and deepest reservoir sandstones are the Santos and Carneros sandstone members of the Temblor Formation. Both sandstones are submarine-fan deposits that are derived from highlands originally located west of the field but now positioned in the Santa Cruz area of coastal California, having been moved northward long the San Andreas fault system (Graham et al., 1989). Deeper sandstone units are present at Elk Hills, including the Eocene Point of Rocks Sandstone Member of the Kreyenhagen Formation, but have failed to produce commercial quantities of oil or gas.

The Monterey Formation contains several productive sandstone units of late Miocene age that are derived from highlands at the eastern and western margins of the basin. The Western 31S and Main Body B sandstones (W31S-MBB; Figure 2) are within the B unit of the Monterey and are part of the much larger Stevens submarine-fan system that extends across much of the Bakersfield arch, northern Maricopa subbasin, and southern Buttonwillow subbasin (MacPherson, 1978; Webb, 1981). The fan was the deep-water extension of the Kern River delta, which was the principal site of deposition of clastics derived from the southern Sierra Nevada. At Elk Hills, the western limit of the Stevens submarine fan falls about midway across the field.

Sands derived from smaller turbidite systems are present at Elk Hills in the A and N units of the Monterey (Figure 2). The 26R and 24Z sand bodies are derived from highlands once present west of Elk Hills but, because of right-lateral faulting on the San Andreas fault, are now located in the Gabilan Range in the central Coast Ranges (Graham, 1978). Both sand bodies were deposited in a slope setting that was disrupted by contemporaneous structural folding. The turbidite systems generally prograded northeastward, but were deflected by growing anticlines and were locally ponded in small synclinal basins before reaching the

floor of the Buttonwillow subbasin (Webb, 1981; Reid, 1990). The result was the deposition of sand bodies along narrow and sinuous fairways in the western area of the field.

Intervals of porcelanite and chert are interbedded with and adjacent to the Stevens sandstone reservoirs. Porcelanite is a diagenetic product derived from deposits of diatom debris. The diagenetic process that forms porcelanite and chert begins with the burial of diatomite and the conversion of unstable amorphous opal (opal A) to cristobalite and tridymite (opal-CT) and, ultimately, to quartz and the formation of porcelaneous and cherty textures (see Isaacs, 1981, for a review of the process). Through this process, porosity is reduced, but even in the quartz phase, is still significant (average 20–25% at Elk Hills; Reid and McIntyre, 2001). Permeability improves during the transition from opal-CT to quartz because the mineral lining the walls of pore throats simplifies, resulting in reduced tortuosity (Reid and McIntyre, 2001; Schwalbach et al., 2001). The CT-quartz transition depth is affected by clay content but occurs at Elk Hills at about 4500 ft (1375 m) subsea.

Pliocene reservoirs of the Elk Hills area consist of sandstone units for the Etchegoin and San Joaquin formations that were deposited in shallow-marine, nearshore, and deltaic-channel environments and represent the final filling of the San Joaquin basin (Reid, 1995). The Calitroleum and Wilhelm sandstone units are poorly sorted, fine-grained sandstones deposited in a lower delta-front environment and are productive in the western area of the field. The Sub-Scalez-1 (SS-1) sandstone is the most significant of the Pliocene reservoirs and consists of coarse-grained sandstone deposited in tidal channels and tidal sand sheets and is present only in eastern Elk Hills. The shallowest and youngest of the Pliocene reservoirs, the Mya interval, consists of numerous narrow sandstone channels that cross the field in a north-south orientation. The Mya channels were deposited by deltas that prograded across the field at the end of the Pliocene.

ELK HILLS FIELD

At the depth of the Stevens reservoirs ($\sim$5000–10,000 ft; $\sim$1500–3000 m subsea), the Elk Hills field contains three elongated domes with steep limbs: the 31S, 29R, and Northwest Stevens anticlines (Figure 4). The overall structural trend is northwest-southeast in the western part of the field and bend to east-west at the east side of the field. Major thrust faults

Table 1. List of Elk Hills Oils Analyzed with Corresponding Reservoir Formation, Age, and Depth as well as Family Designation*

Sample ID	Family**	Field	Well	Formation	Age	Depth (ft)	$<C_{15}$
CA230	SOZ	Elk Hills	37-35R	Wilhelm 1A, 1B	Pliocene	2794	37.6
CA231	SOZ	Elk Hills	153H-36R-RD2	CAL 1	Pliocene	4701	65.1
CA232	SOZ	Elk Hills	38H-31S	Gusher 4	Pliocene	2530	82.0
CA233	SOZ	Elk Hills	3-56-24Z	Sub Mulinia	Pliocene	2423	71.6
CA234	SOZ	Elk Hills	28-35R	Sub Mulinia	Pliocene	2530	46.0
CA235	SOZ	Elk Hills	86-24R	Sub Mulinia	Pliocene	2915	49.8
CA236	SOZ	Elk Hills	43-24Z	Wilhelm	Pliocene	2257	65.0
CA237	SOZ	Elk Hills	37-28R	Gusher 4	Pliocene	2999	60.2
CA238	SOZ	Elk Hills	34S-36R	CAL 2	Pliocene	4098	63.5
CA239	SOZ	Elk Hills	357XH-30S	Above bitumen (2)	Pliocene	2589	31.1
CA240	SOZ	Elk Hills	57-28R	Wilhelm 1A, 1B, 2	Pliocene	2387	67.0
CA258	SOZ	Elk Hills	312-31S	C4D-CT Phase	Pliocene	3692	58.5
CA260	SOZ	Elk Hills	376-24Z	Mid Reefridge-CT/Qtz	Upper Miocene–Pliocene	5145	50.4
CA197	SOZ	Elk Hills	58A-25R	Reef Ridge/C4D	Upper Miocene–Pliocene	3600	57.7
CA263	SOZ		35NE-6G				42.5
CA021	B1	Elk Hills	583L-30R	Lower Santos	Lower Miocene	9500	24.1
CA210	B1	Elk Hills	584-26Z	Carneros	Lower Miocene	8700	77.7
CA212	B1	Elk Hills	583L-30R	Santos	Lower Miocene		25.8
CA213	B1	Elk Hills	934H-29R RD4	Santos	Lower Miocene	9600	22.4
CA223	B1	Elk Hills	578-24Z	Carneros	Lower Miocene	9100	60.0
CA224	B1	Elk Hills	542-30R	Carneros	Lower Miocene	8500	59.9
CA015	B1+	Elk Hills	18-14Z	Temblor (+?)	Middle Miocene	8000	40.4
CA022	C	Elk Hills	362H-7R	Stevens NWS	Upper Miocene	9100	36.0
CA203	C	Elk Hills	331H-18R	A-1	Upper Miocene	9400	40.2
CA204	C	Elk Hills	373AH-7R	A-2	Upper Miocene	9160	33.7
CA205	C	Elk Hills	324H-7R	A1/A2	Upper Miocene	6100	58.3
CA206	C	Elk Hills	318-8R	A4/5	Upper Miocene	8900	31.8
CA011	A1	Elk Hills	372-17R	Stevens NWS	Upper Miocene	8900	41.8
CA016	A1	Elk Hills	362-24Z	Stevens 24Z	Upper Miocene	5800	42.4
CA017	A1	Elk Hills	362-16R	Stevens NWS	Upper Miocene	8600	41.9
CA025	A1	Elk Hills	312H-26R	Stevens 26R	Upper Miocene	6500	49.6
CA207	A1	Elk Hills	313H-16H	A5/6	Upper Miocene	8540	44.8
CA208	A1	Elk Hills	372-17R	A5/6	Upper Miocene	8850	43.9
CA214	A1	Elk Hills	324-15R	Stevens NWS (T3/4)	Upper Miocene	8800	50.8
CA215	A1	Elk Hills	334-15R	Stevens NWS (T3/4)	Upper Miocene	8800	47.8
CA217	A1	Elk Hills	328-35R-RD1	Stevens 2B	Upper Miocene	6300	53.5
CA218	A1	Elk Hills	317X-13Z	Stevens N Shale	Upper Miocene	5500	44.7
CA198	A2	Elk Hills	381-36S	UMBB	Upper Miocene	8600	98.3
CA199	A2	Elk Hills	383H-36S RD2	UMBB	Upper Miocene	8750	42.0
CA200	A2	Elk Hills	333-35S	UMBB	Upper Miocene	7350	44.8
CA202	A2	Elk Hills	315-35S	UMBB	Upper Miocene	7000	45.0
CA209	A2	Elk Hills	384H-25R	NA/ND	Upper Miocene	5250	58.4
CA216	A2	Elk Hills	346-35R	Stevens 2B	Upper Miocene	6500	48.7
CA219	A2	Elk Hills	383-26Z	Stevens	Upper Miocene	5500	38.9
CA220	A2	Elk Hills	352-26Z	Stevens	Upper Miocene	5800	32.4
CA012	SH	Elk Hills	361-25S	Stevens MBB	Upper Miocene	9700	40.4
CA013	SH	Elk Hills	343-29R	Stevens D Shale	Middle Miocene	6000	42.2
CA014	SH	Elk Hills	324-4G	Stevens A	Upper Miocene	6400	44.1

API	% S	Ni/V	% Sat	% Aro	% Asph	S/A	$^{13}C_s$†	$^{13}C_a$†	$^{13}C_{wo}$†	^{13}C LE††	^{13}C HE††
27.2	1.12	4.5	28.4	38.7	3.5	0.73	−25.12	−24.37	−24.27	−23.75	−24.58
39.1	0.68	4.3	30.7	35.1	5.2	0.87	−25.40	−24.43	−24.10	−23.76	−24.73
48.2	0.40	1.8	33.0	34.0	5.7	0.97	−25.24	−24.68	−23.85	−23.63	−24.86
36.4	0.58	2.6	30.6	37.5	5.5	0.82	−25.27	−24.43	−24.13	−23.91	−24.69
28.1	1.04	4.7	28.3	39.4	3.1	0.72	−25.18	−24.34	−24.04	−23.41	−24.58
15.8	0.80	3.1	24.0	41.9	6.1	0.57	−24.97	−24.34	−24.09	−23.69	−24.49
39.4	0.72	4.9	32.3	35.5	2.9	0.91	−25.26	−24.50	−24.13	−23.80	−24.75
36.7	0.84	3.8	31.7	34.9	4.3	0.91	−25.49	−24.53	−24.29	−23.93	−24.83
39.0	0.65	3.6	31.8	35.1	6.4	0.91	−25.35	−24.33	−24.03	−23.67	−24.65
14.3	1.10	5.0	27.6	38.0	4.5	0.73	−25.24	−24.41	−24.30	−23.55	−24.64
38.1	0.69	3.7	30.4	35.1	3.2	0.87	−25.46	−24.41	−24.18	−23.91	−24.73
36.3	0.73	2.1	33.1	38.6	3.3	0.86	−25.55	−24.45	−24.26	−23.87	−24.81
35.5	0.91	2.3	32.9	38.7	2.1	0.85	−25.19	−24.39	−24.07	−23.50	−24.65
38.6	0.74	5.8	33.3	38.4	2.1	0.87	−25.41	−24.30			−24.67
28.8	1.04	4.8	26.0	39.6	4.8	0.66	−25.14	−24.32	−24.22	−23.80	−24.53
27.6	0.48	3.2	34.2	39.2	5.6	0.87	−24.62	−23.56	−24.04	−24.41	−23.92
50.0	0.20	3.5	45.7	35.7	1.9	1.28	−24.82	−23.68	−23.53	−23.34	−24.20
27.6	0.45	3.3	31.6	39.2	7.1	0.81	−24.68	−23.56	−23.76	−23.32	−23.91
	0.65	2.8	7.5	11.4	28.9	0.66	−24.13	−23.12	−23.27	−23.53	−23.20
35.9	0.34	5.0	40.6	36.6	6.6	1.11	−24.95	−23.64	−23.84	−23.62	−24.17
36.3	0.32	7.8	41.8	35.1	5.9	1.19	−25.11	−23.65	−23.84	−23.56	−24.26
35.2	0.92	1.8	38.8	33.8	4.2	1.15	−25.11	−23.82	−24.10	−23.77	−24.32
37.7	1.51	1.0	29.6	38.9	5.7	0.76	−24.96	−23.63	−23.58	−23.33	−24.02
26.7	1.39	0.5	24.5	38.8	15.5	0.63	−24.87	−23.57	−23.54	−23.31	−23.89
14.0	0.65	0.3	22.2	33.1	22.5	0.67	−24.94	−23.52	−23.25	−22.95	−23.84
24.5	0.79	0.4	25.5	37.6	12.4	0.68	−24.98	−23.62	−23.59	−23.06	−23.97
	1.00	0.7	33.1	38.5	8.6	0.86	−24.54	−23.24	−23.32	−23.16	−23.67
35.4	0.70	0.3	39.6	33.1	3.8	1.20	−24.15	−22.78	−23.04	−22.65	−23.32
35.0	0.68	0.6	50.9	31.4	1.7	1.62	−24.75	−23.12	−23.45	−22.77	−23.95
36.8	0.53	0.3	38.3	33.4	6.3	1.15	−24.38	−23.08	−23.22	−22.72	−23.58
40.8	0.62	0.6	40.5	35.3	7.0	1.15	−24.28	−23.12	−23.34	−23.09	−23.59
33.4	0.59	0.7	43.4	36.5	4.2	1.19	−24.02	−22.78	−22.98	−22.56	−23.32
34.8	0.71	0.6	41.4	37.0	4.7	1.12	−24.14	−22.80	−23.02	−22.59	−23.35
38.0	0.43	5.3	47.5	32.0	5.4	1.48	−24.14	−22.76	−23.21	−23.01	−23.42
33.1	0.54	0.4	43.7	34.9	4.1	1.25	−24.20	−22.84	−23.13	−22.80	−23.43
38.1	0.41	16.0	49.5	30.8	1.3	1.61	−24.49	−23.15	−23.55	−23.32	−23.81
30.8	1.17	2.2	32.1	34.0	5.8	0.94	−24.65	−23.59	−23.57	−23.12	−23.93
60	0.02	1.8	40.4	35.9	0.0	1.13	−24.73	−23.54	−20.28	−20.22	−24.02
33.5	0.68	1.8	39.4	37.3	4.0	1.06	−24.79	−23.45	−23.84	−23.65	−23.98
33.0	0.62	1.4	42.5	35.5	3.3	1.20	−24.74	−23.35	−23.71	−23.43	−23.94
34.0	0.47	1.9	44.8	36.0	3.2	1.24	−24.61	−23.31	−23.70	−23.46	−23.89
39.7	0.65	4.4	38.8	33.0	2.2	1.18	−25.04	−23.97	−23.91	−23.57	−24.39
32.8	0.49	13.5	42.2	35.2	5.2	1.20	−24.48	−23.30	−23.54	−23.27	−23.80
32.9	0.64	2.6	41.6	34.6	3.0	1.20	−24.47	−23.39	−23.56	−23.12	−23.84
30.6	0.76	0.9	43.4	32.4	3.3	1.34	−24.45	−23.29	−23.62	−23.26	−23.79
32.7	0.73	1.1	32.9	35.2	4.7	0.93	−24.69	−23.36	−23.41	−22.84	−23.80
38.4	0.48	0.8	46.1	31.4	3.7	1.47	−24.47	−23.18	−23.99	−24.28	−23.77
39.0	0.49	1.0	48.3	34.1	1.4	1.42	−24.93	−23.36	−23.67	−23.10	−24.12

Table 1. Continued

Sample ID	Family**	Field	Well	Formation	Age	Depth (ft)	$<C_{15}$
CA018	SH	Elk Hills	347-33S	Stevens MBB	Upper Miocene	6600	45.8
CA019	SH	Elk Hills	388-28R	Stevens B	Upper Miocene	6500	46.4
CA020	SH	Elk Hills	337HA-33S	Stevens MBB	Upper Miocene	6600	45.5
CA023	SH	Elk Hills	325H-30S	Stevens D Shale	Middle Miocene	6900	52.4
CA024	SH	Elk Hills	348A-23R	Stevens W.31S	Upper Miocene	6400	45.9
CA201	SH	Elk Hills	347-35S	UMBB	Upper Miocene	7300	55.8
CA246	SH	Elk Hills	322H-32S	A-Sand	Upper Miocene	5094	50.8
CA247	SH	Elk Hills	371X-32R	N-CT Phase	Upper Miocene	5457	45.8
CA248	SH	Elk Hills	314-5G	N-Qtz Phase	Upper Miocene	6345	48.4
CA249	SH	Elk Hills	326-19R	N-Qtz Phase	Upper Miocene	5690	51.6
CA250	SH	Elk Hills	326-29R	N-Qtz Phase	Upper Miocene	5600	46.8
CA251	SH	Elk Hills	382H-5G	A-Sand	Upper Miocene	6306	48.8
CA252	SH	Elk Hills	314-3G	N-Qtz Phase	Upper Miocene	6660	44.8
CA253	SH	Elk Hills	368H-19R	N-CT Phase	Upper Miocene	5250	47.1
CA254	SH	Elk Hills	357-35S	N-Qtz Phase	Upper Miocene	5695	67.7
CA255	SH	Elk Hills	386XH-33S	A-Sand	Upper Miocene	6849	46.0
CA256	SH	Elk Hills	321XH-33R	B-Qtz Phase	Upper Miocene	5398	45.0
CA257	SH	Elk Hills	382-25Z	Olig/C4D-CT?	Upper Miocene	4910	49.7
CA259	SH	Elk Hills	325-28R	B-Qtz Phase	Upper Miocene	5550	48.5
CA225	KH	Kettleman N. Dome	E72-33J	Kreyenhagen	Eocene	9400	47.1
CA226	KH	Kettleman N. Dome	341-11P	Kreyenhagen	Eocene	8850	47.5
CA228	KH	Belgian Anticline	75-17Y	Point of Rocks III	Eocene	2300	86.3
CA227	~A1	West Bellevue	Lovegren 62X-32	Lower Stevens	Miocene	8815	39.9
CA229	High mat.	Ekho	1	Temblor	Oligocene	18,015	63.9
CA221	Biodeg.	Deer Creek	Community lease		Miocene	800	7.2
CA245	Biodeg.	Midway-Sunset					41.3
OXCA001	~SOZ	Kern River	Apollo-CP-Revenue	Vedder Sands	Oligocene	4800	44.1
OXCA002	~B1	Rio Bravo	Mandell 2 (RD1)	Freeman-Jewette Fm.	Miocene	11,260	47.1
OXCA003	~SOZ	Kern River	Revenue 4X	Vedder Sands	Oligocene	4700	43.7

*Column definitions: $<C_{15}$ = % less than C_{15} (light ends); S/A = C_{15+} saturated hydrocarbons/C_{15+} aromatic hydrocarbons; $^{13}C_s$ = carbon isotope composition of C_{15+} saturated hydrocarbons; $^{13}C_a$ = carbon isotope composition of C_{15+} aromatic hydrocarbons; $^{13}C_{wo}$ = carbon isotope composition of whole oil; ^{13}C LE = calculated carbon isotope composition of light-end components; ^{13}C HE = calculated carbon isotope composition of heavy ends.

**For explanation see text section titled Oil Families Description.

†Measured.

††Calculated.

are present on the flanks of all the anticlines and generally parallel to the fold axes (Imperato, 1995; Fiore et al., 2004). Most thrust faults terminate upward in the thick shale sequence that separates the Monterey and Etchegoin reservoirs. At the depth of the Pliocene sandstone section (about 2000–5000 ft [600–1500 m] subsea), the 29R and 31S anticlines merge to form a single large structure that generally has an east-west trend. The Northwest Stevens anticline did not have significant activity following the end of the Miocene and does not make a major contribution to the Pliocene structure. The Pliocene section in eastern Elk

Hills is broken by numerous northeast-southwest–trending normal faults. The Elk Hills anticlinal complex is most likely a fault propagation fold formed by north- and northeast-directed compression (Imperato, 1995; Fiore et al., 2004). Like many of the west-side anticlines, folding began at Elk Hills in late Miocene, accelerated in the Pliocene, and continues today (Harding, 1976).

Elk Hills has produced more than 1.2 billion bbl oil and 1.6 tcf gas (California Division of Oil, Gas, and Geothermal Resources, 2003) from four petroleum zones. The Carneros zone includes the Santos

API	% S	Ni/V	% Sat	% Aro	% Asph	S/A	$^{13}C_s$†	$^{13}C_a$†	$^{13}C_{wo}$†	^{13}C LE††	^{13}C HE††
38.5	0.42	0.9	46.7	33.8	2.1	1.38	−24.57	−23.30	−23.70	−23.47	−23.89
37.7	0.40	0.8	49.5	30.4	1.8	1.63	−24.35	−23.08	−23.55	−23.37	−23.71
39.2	0.39	1.0	47.7	32.0	1.8	1.49	−24.55	−23.26	−23.71	−23.51	−23.88
33.6	0.44	1.6	45.1	32.9	2.4	1.37	−24.77	−23.50	−24.00	−23.93	−24.07
38.8	0.42	0.9	48.9	32.0	2.8	1.53	−24.43	−23.18	−23.61	−23.40	−23.79
21.1	0.47	1.7	24.2	25.8	8.7	0.94	−24.71	−23.41	−23.80	−23.86	−23.72
34.5	0.78	1.8	37.0	36.7	3.3	1.01	−24.95	−23.83	−23.97	−23.70	−24.24
30.6	0.54	1.6	45.6	35.7	2.8	1.28	−24.53	−23.30	−23.67	−23.44	−23.86
36.0	0.61	1.7	41.6	37.5	3.0	1.11	−24.66	−23.36	−23.67	−23.42	−23.90
37.7	0.52	1.4	43.4	34.7	3.3	1.25	−24.53	−23.38	−23.64	−23.42	−23.88
37.8	0.56	1.6	44.5	33.8	2.5	1.32	−24.49	−23.28	−23.63	−23.42	−23.82
37.7	0.55	1.4	44.6	35.7	2.9	1.25	−24.63	−23.49	−23.77	−23.53	−24.00
34.2	0.92	1.8	32.2	36.7	6.2	0.88	−24.62	−23.42	−23.41	−22.92	−23.81
36.0	0.70	1.5	41.3	33.7	3.1	1.23	−24.57	−23.54	−23.70	−23.40	−23.97
40.9	0.40	1.4	46.8	30.0	9.8	1.56	−24.60	−23.50	−23.50	−23.25	−24.01
35.1	0.47	1.4	49.5	33.8	2.6	1.46	−24.83	−23.35	−23.69	−23.23	−24.08
34.2	0.46	1.0	47.5	34.2	2.3	1.39	−24.41	−23.15	−23.53	−23.26	−23.75
36.3	0.79	1.8	38.4	37.5	1.9	1.02	−24.91	−23.87	−23.85	−23.42	−24.27
36.9	0.44	1.0	49.4	34.6	1.9	1.43	−24.47	−23.22	−23.58	−23.31	−23.84
36.6	0.39	3.2	45.7	37.0	1.6	1.23	−29.07	−28.19	−28.64	−28.68	−28.59
37.8	0.37	3.8	45.6	37.3	1.8	1.22	−28.83	−27.94	−28.45	−28.54	−28.35
41.7	0.06	9.0	51.2	36.8	0.0	1.39	−28.03	−25.97	−26.56	−23.64	−27.02
35.7	0.72	1.9	42.8	35.4	3.9	1.21	−24.64	−23.45	−23.82	−23.73	−23.96
37.7	0.19	3.0	50.5	38.0	0.3	1.33	−23.75	−22.40	−23.19	−23.38	−23.08
13.0	0.43	3.5	43.3	41.5	0.9	1.04	−26.49	−25.55	−25.94	−25.94	−25.96
13.9	0.92	0.8	16.0	35.8	6.9	0.45	−24.44	−23.52			−23.67
30.2	0.70	5.7	39.8	36.8	6.0	1.08	−25.08	−23.64	−23.70	−23.30	−24.21
35.1	0.33	5.5	46.5	37.6	2.7	1.24	−24.67	−23.47	−23.96	−23.88	−24.03
31.9	0.71	9.2	40.0	36.6	6.1	1.09	−25.02	−23.61	−23.78	−23.47	−24.17

and Carneros sandstones and contains light-gravity oil, condensate, and gas and is productive only on the 29R anticline at depths of about 10,000 ft (3048 m). The Stevens oil zone contains several major pools in structural and stratigraphic traps on each of the large anticlines. Drill depth of pools ranges from 5000 to 10,000 ft (1500 to 3000 m), with many wells completed in oil columns originally 500–1000 ft (152–305 m) thick. Produced oil from all Stevens pools averages 35° API, with abundant associated produced gas. The shallow oil zone produces from drill depths of 2000–4000 ft (610–1220 m) and produces light-gravity oil and gas from the Calitroleum and Wilhelm reservoirs in western Elk Hills and 25–30° API oil in the SS-1 reservoir on the east side of the field. The dry gas zone, as its name implies, produces only methane from the Pliocene Mya interval at drill depths of 1000–2000 ft (305–610 m).

EXPERIMENTAL METHODS

Standard laboratory procedures were followed in obtaining the geochemical results used in the multivariate statistical analysis and are summarized here.

The weight of the light ends lost from each oil sample under a stream of nitrogen was determined gravimetrically ($<C_{15+}$). The amount of asphaltenes was measured by precipitation using n-hexane (overnight at room temperature). The C_{15+} deasphalted fractions were separated into saturated hydrocarbon, aromatic hydrocarbon, and nitrogen-sulfur-oxygen compounds or resin fractions using gravity-flow column chromatography employing a 100–200 mesh silica gel support activated at 400°C prior to use. Hexane was used to elute the saturated hydrocarbons; dichloromethane was used to elute the aromatic hydrocarbons; and dichloromethane/methanol (50:50) was used to elute the nitrogen-sulfur-oxygen fraction. Following solvent

Figure 2. Stratigraphic section and oil families at Elk Hills. For explanation of oil families, see text section titled Oil Families Description.
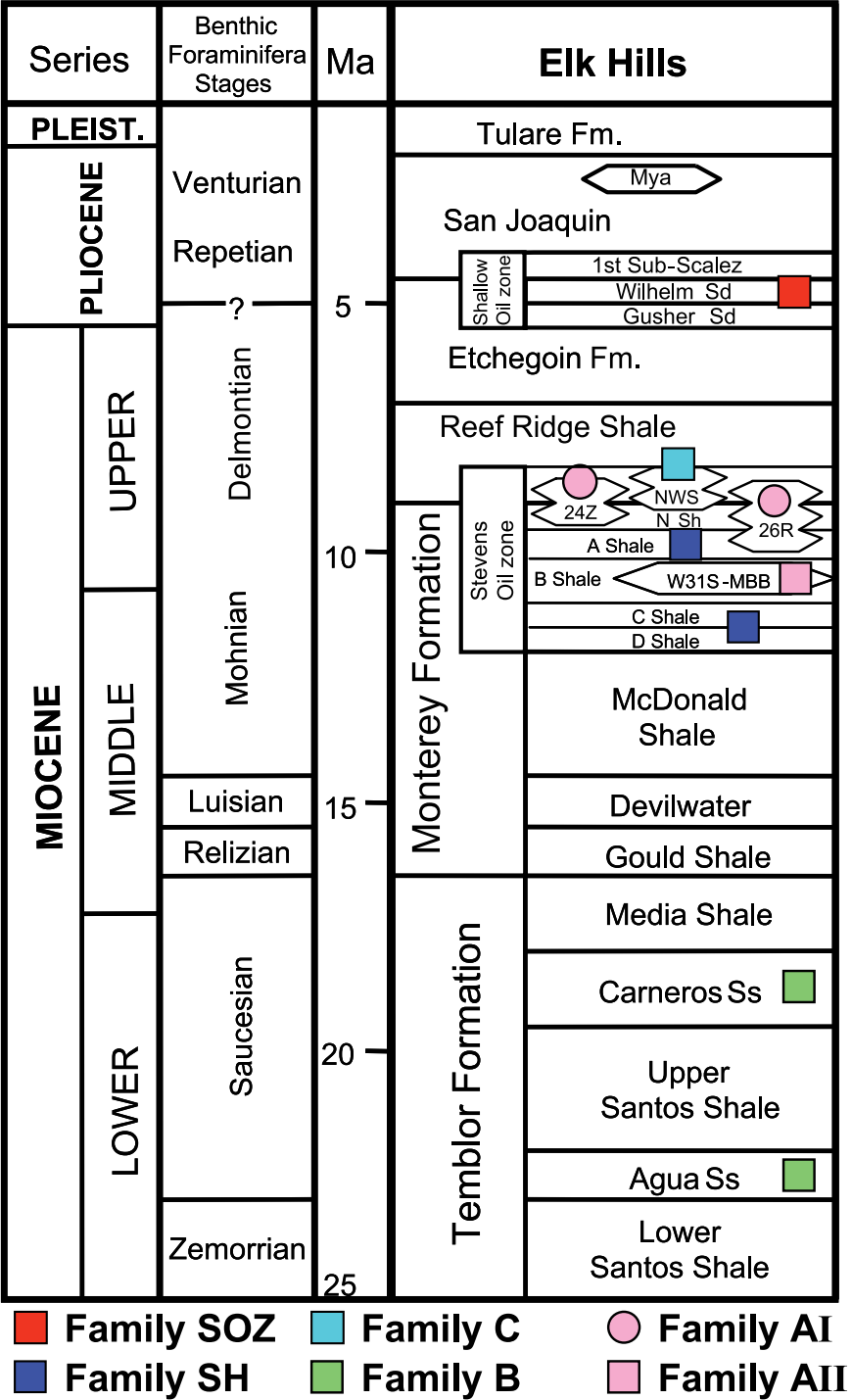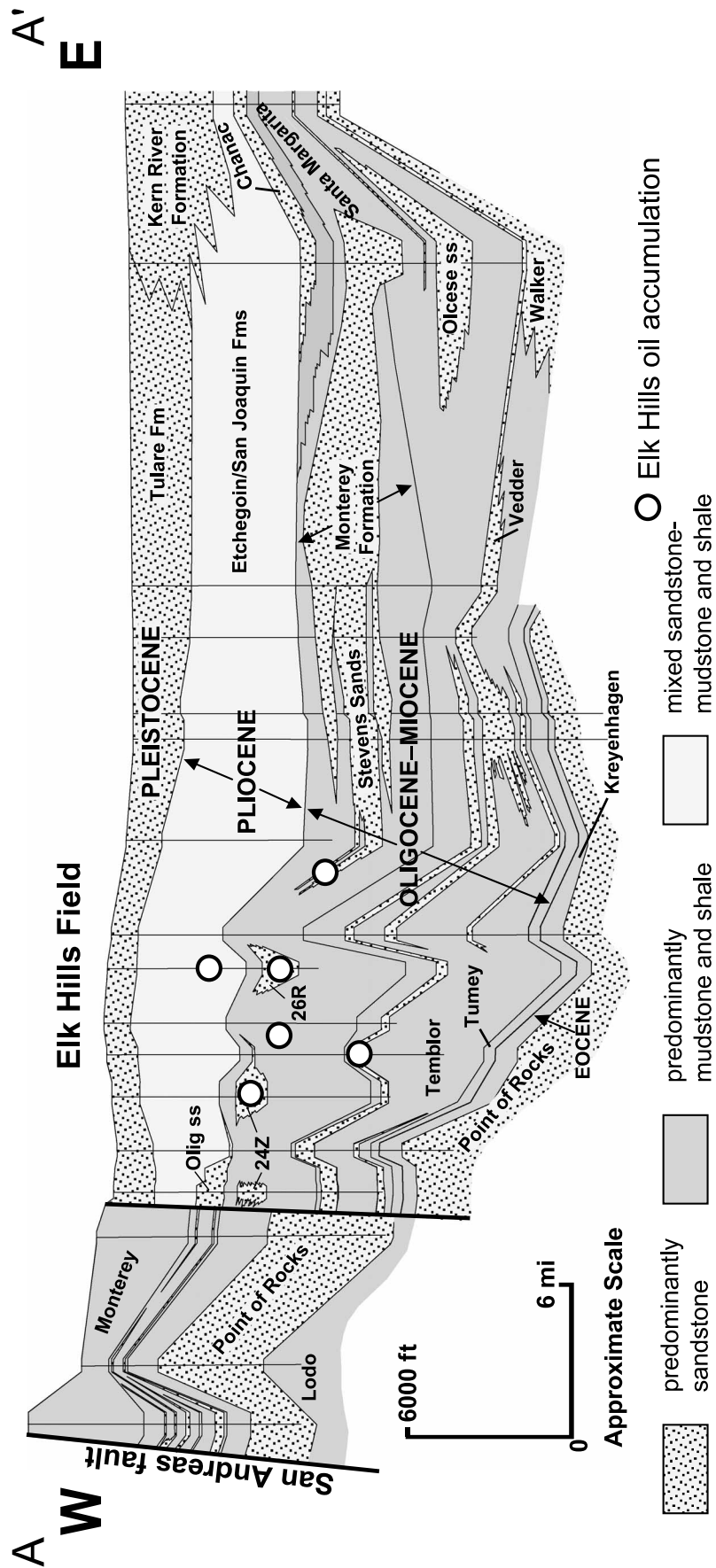
Figure 3. Cross section of the southern San Joaquin basin from the San Andreas fault through Elk Hills to the Sierra Nevada. Modified from Dunwoody (1986).
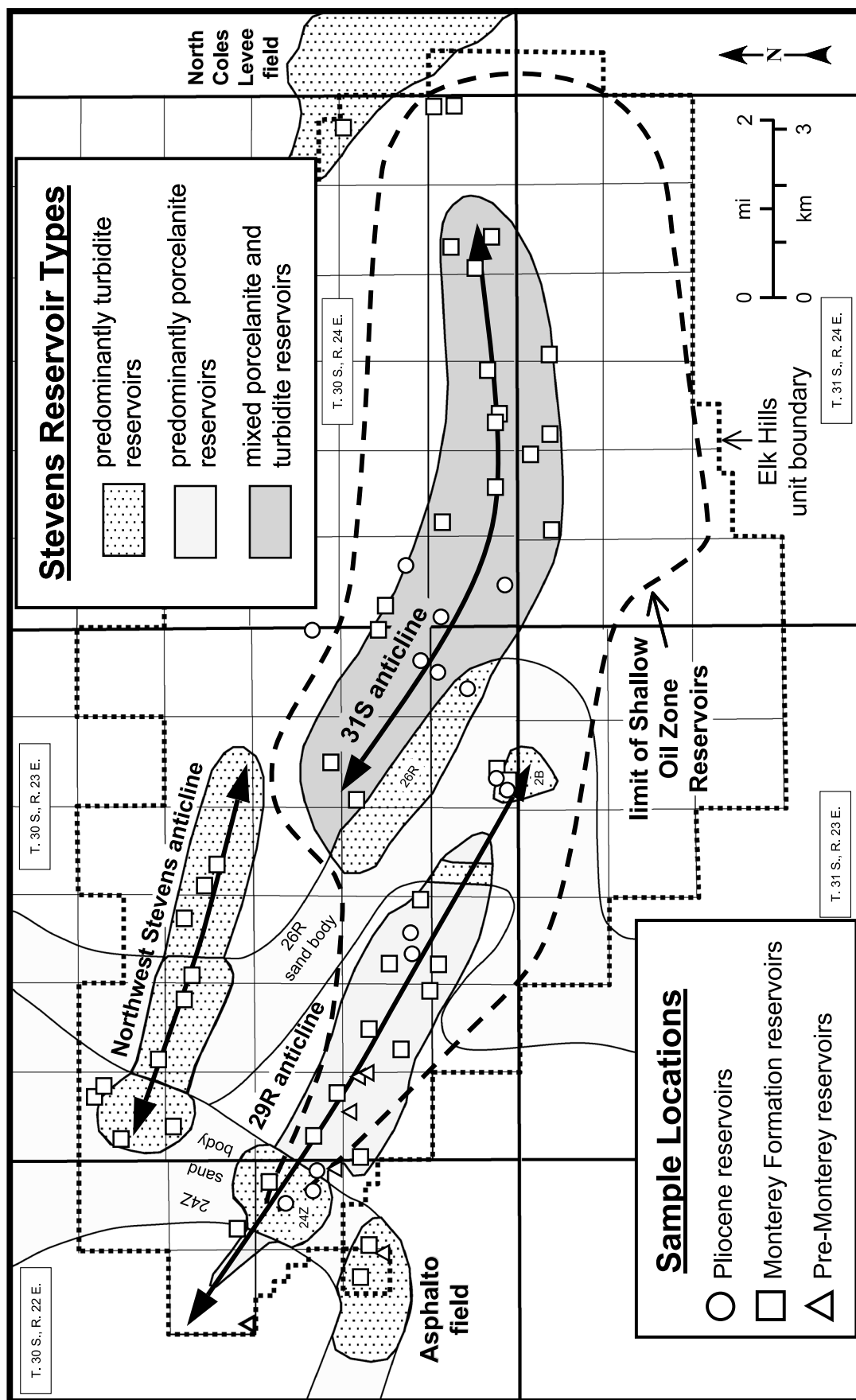
Figure 4. Detailed map of the Elk Hills field showing location of geochemical samples, location of the major Stevens reservoirs, and a general outline of the shallow oil zone. Some samples are from minor reservoirs that have unmapped aerial distributions.

evaporation, the recovered fractions were quantified gravimetrically. The C_{15+} saturated hydrocarbon fraction was subjected to molecular sieve filtration (Union Carbide S-115 powder) after the technique described by West et al. (1990) to concentrate the branched and cyclic biomarker fractions. Stable carbon isotopic compositions of the whole oil as well as the C_{15+} saturated and aromatic hydrocarbon fractions were determined using the combustion technique of Sofer (1980) and a Finnigan delta E isotope ratio mass spectrometer. Results are reported relative to the Peedee belemnite standard.

Whole crude oils were injected (split mode 70:1) on a 30-m × 0.32-mm (100-ft × 0.012-in.) J&W DB-5 column (0.2-μm film thickness) and temperature programmed from −60 to 350°C at 12°C/min using a Hewlett Packard 5890 gas chromatograph. Helium was used as the carrier gas. Gas chromatographic and mass spectrometric analyses of C_{15+} branched/cyclic and aromatic hydrocarbon fractions (to determine sterane and terpane biomarker distributions and quantities) were performed using a Hewlett Packard 5890 gas chromatograph (split injection) interfaced to a HP 5971 mass spectrometer. The HP-2 column (50 m × 0.2 mm [164 ft × 0.0078 in.]; 0.11-μm film thickness) was temperature programmed from 150 to 325°C at 2°C/min for branched and cyclic hydrocarbons and 100 to 325°C at 3°C/min for aromatics. The mass spectrometer was run in the selected ion mode, monitoring ion mass-to-charge ratio (m/z) 177, 191, 205, 217, 218, 221, 231, and 259 (branched/cyclic) and m/z 133, 178, 184, 192, 198, 231, 245, and 253 (aromatics). To determine absolute concentrations of individual biomarkers, a deuterated internal standard (d4-C29 20R sterane; Chiron Laboratories, Norway) was added to the C_{15+} branched and cyclic hydrocarbon fraction. Response factors (RF) were determined by comparing the mass spectral response at m/z 221 for the deuterated standard to hopane (m/z 191) and sterane (m/z 217) authentic standards. These response factors were found to be approximately 1.4 for terpanes and 1.0 for steranes. Concentrations of individual biomarkers in the branched and cyclic fraction were determined using the following equation:

Concentration(ppm)
= [(peak height of biomarker)(nanograms of standard)]
/[(peak height of standard)(RF)
× (milligrams of branched and cyclic fraction)]

OIL FAMILIES DESCRIPTION

Table 1 lists the Elk Hills wells that produced the 66 oils used in this study and provides reservoir identification and depth, as well as bulk properties such as API gravity and stable carbon isotope compositions. Figure 4 shows a map locating the samples, highlighting the Elk Hills oils from pre-Monterey reservoirs (7 samples) as well as 14 samples from the Pliocene shallow oil zone. A total of 32 samples come from the various Stevens turbidites, and 13 samples are from porcelanite reservoirs (Elk Hills Shale Member of the Monterey Formation). The Elk Hills samples are evenly distributed between the two main producing anticlines: 31S (eastern Elk Hills) and 29R (western Elk Hills), with 10 oils from the Northwest Stevens anticline. Complete analytical results of all the oils used in this study, including whole oil chromatograms and terpane and sterane biomarker distributions and concentrations, can be accessed from the GeoMark Research Reservoir Fluid Database (www.RFDbase.com) using the demo-user password.

Also shown in Table 1 are the results of the oil classification or groupings (oil families), which will be described in detail below. Family member oils generally share a common source organofacies, albeit at different levels of thermal maturity. Most remarkably, Elk Hills oil families strongly correlate to reservoir horizon (see stratigraphic section, Figure 2), although all Elk Hills oils were generated from the Monterey, even family B oils that produce from pre-Monterey horizons.

Statistical Analyses

The two statistical treatments used in the present study to delineate the different oil families are termed principal component analysis and hierarchical cluster analysis and were performed using computer programs from Infometrix (Pirouette™). In principal component analysis, new independent variables are created (i.e., principal components) that are linear combinations of the original variables (i.e., geochemical parameters). The primary objective of the principal component analysis is to reduce the dimensionality of the data to a few important components that best explain the variation in the data. Oil samples can be plotted in a principal component space, for example, PC1 (factor 1) versus PC2 (factor 2), like any other x-y plot. This is called a scores plot. The geochemical variables

responsible for the PC axes can be viewed as a loadings plot. Hierarchical cluster analysis is an ancillary technique to principal component analysis where a distance matrix is created from the scaled data. A resulting dendrogram is the output of a cluster analysis and shows groups or clusters of related oils. The distance between any two samples on a hierarchical cluster analysis is a measure of their similarity. (This distance is similar to a linear correlation coefficient; perfect correlation would have a value of 1.0, whereas poor correlation would have values less than 0.5.)

The geochemical variables used to correlate oils are various source-dependent biomarker ratios and stable carbon isotopic compositions. Biomarkers (biological markers) are geochemical fossils and are defined as organic compounds found in sedimentary rocks or oils in which a sufficient part of the carbon skeleton has been preserved. These compounds, including terpanes and steranes, can be correlated with the original biochemical precursor after having undergone accumulation, diagenesis, and catagenesis (i.e., oil generation). Thus, biomarkers can be indicators of source rock depositional environments in the same manner that the physical remains of organisms can describe depositional systems. Biomarkers are also useful as thermal-maturity indicators. A good review of biomarkers and their applications in petroleum geochemistry can be found in Peters et al. (2005).

The level of statistical correlation between the 66 oils included in the Elk Hills data set is shown in the hierarchical cluster analysis dendrogram presented in Figure 5. Eighteen isotope and biomarker variables (identified in Figure 6) were used to construct the cluster analysis dendrogram. Five compositional clusters are identified on the dendrogram:

family A: Stevens turbidites; includes closely related subfamilies AI and AII
family B: oils in pre-Monterey reservoirs
family C: limited to the Stevens zone in the 7R area of the Northwest Stevens anticline
family SH: oils from the Stevens porcelanite reservoirs
family SOZ: oils from the Pliocene shallow oil zone

The analytical variation in the data set is minimal. For example, oil samples CA011 and CA208 (well 372-17R; family AI) as well as CA021 and CA212 (well 583L-30R; family B) represent duplicate pairs. Although samples CA208 and CA212 were analyzed 1.5 yr after samples CA011 and CA021, both duplicate pairs are highly correlative, remaining within

their respective oil family. This indicates little variation caused by analytical techniques. Temblor oil sample CA015 (well 18-14Z) is probably a member of both families B and A (instead of the family SOZ) because it is likely a comingled oil, representing both pre-Monterey and Stevens reservoirs (B. Countryman, 2000, personal communication).

Figure 6 shows the results of the principal component analysis using the heavy-end carbon isotope composition of the saturated and aromatic hydrocarbon fractions and key source-related biomarker ratios shown on the variable (loadings) plot. These are the same geochemical variables used in the cluster analysis. The five families defined in the cluster analysis are labeled on the principal component plot (A, B, C, SOZ, and SH) using the same color code. By comparing the scores and loadings plot, the geochemical variables responsible for the groupings become apparent. For example, the SOZ oils have high negative factor 1 values, meaning that they have the highest %C_{29} variable (steranes mostly from green algae) and the lightest (i.e., most negative) carbon isotope values ($^{13}C_s$ and $^{13}C_a$). Family B oils, from pre-Monterey reservoirs, have high S1/S6 (rearranged to regular steranes) and low C_{28}/H (bisnorhopane to hopane) ratios, whereas family C oils from the Northwest Stevens anticline have reversed values. These two parameters are most affected by thermal maturity, suggesting that the C_{15+} oil components in family B come from more deeply buried Monterey facies than family C oils. Families A and SH are not readily distinguished using only factors 1 and 2. These two families, which represent most of the oil produced from Elk Hills, are also most closely related based on the cluster analysis (Figure 5). By rotating the principal component axis (Figure 6), family A is better separated from family SH. Not surprisingly, the porcelanite-reservoired oils (SH) contain slightly more C_{28} steranes (%C_{28}), many of which originate from diatoms.

Oils from Other Fields

Table 1 also lists 10 oils from southern San Joaquin fields other than Elk Hills. Three of these oils (CA225, CA226, and CA228) are from Eocene reservoirs (Kettleman N. Dome and Belgian Anticline fields) and have very light carbon isotopic compositions highly suggestive of Kreyenhagen source rocks (Peters et al., 1994). The two Kern River oils (CA269 and CA271) statistically most resemble the Elk Hills SOZ family,
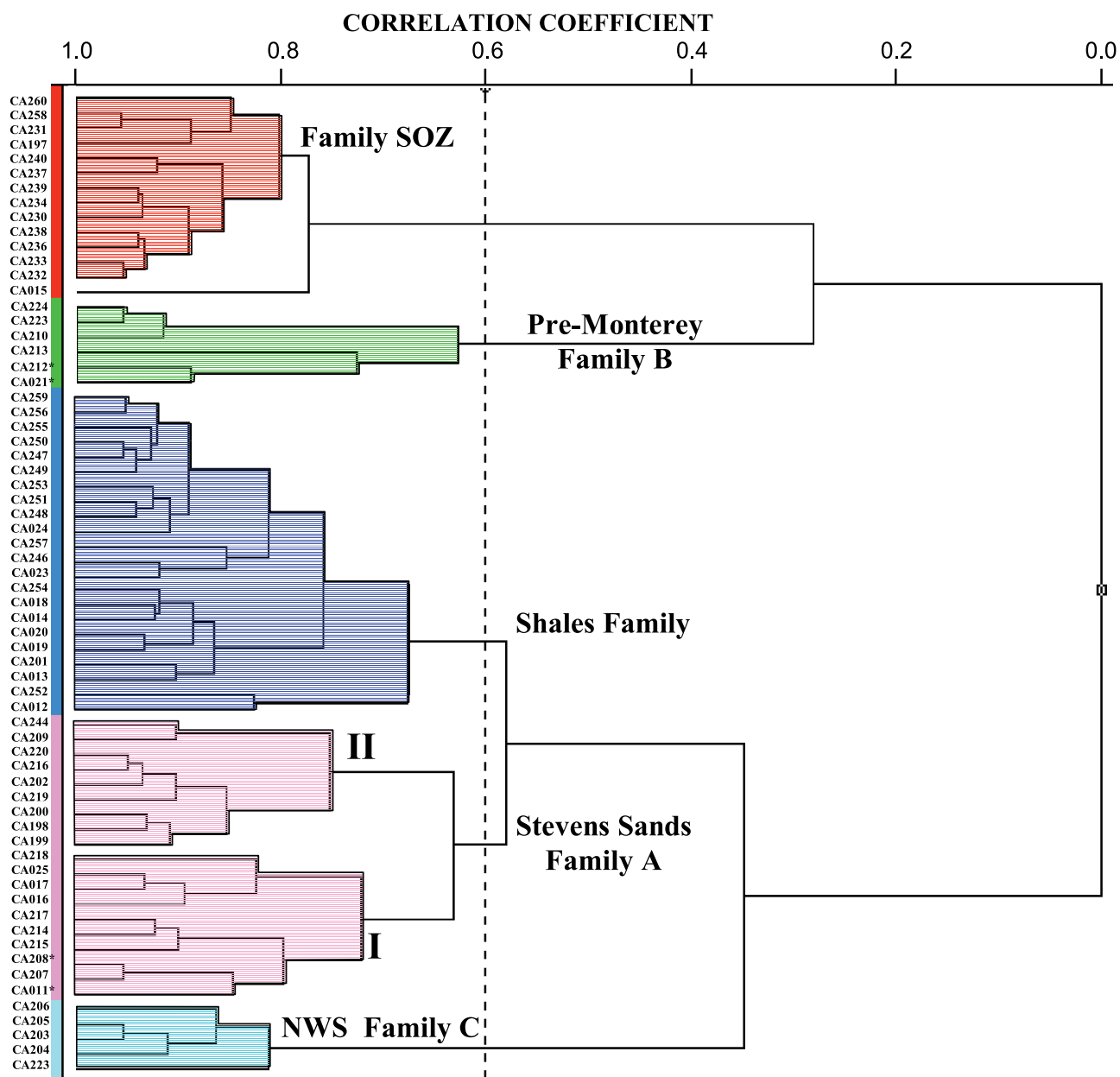
Figure 5. Cluster analysis dendrogram showing the five principal Elk Hills oil families. The geochemical variables used to construct this dendrogram are defined in Figure 6. Oils CA212 and CA021 as well as CA208 and CA011 represent duplicate sample pairs, collected and analyzed 18 months apart; the high correlations indicate little variation caused by sampling or analytical technique.

although they are produced from the Oligocene Vedder sandstone. The Stevens oil from West Bellevue (CA227) correlates best with family AI (same as Elk Hills Stevens oils), whereas the Rio Bravo oil (CA270) appears to be a member of family B. Heavily biodegraded oils from Midway-Sunset (CA245) and Deer Creek (CA221) fields preclude accurate correlation with Elk Hills families because the steranes have been degraded. The carbon isotopes, however, suggest a Monterey origin for oil from the Midway-Sunset field and perhaps a mixed Miocene–Eocene origin for Deer Creek oil. The deep Temblor test from exploratory well Ekho 1 (CA229) is too mature (the terpanes and steranes have been thermally degraded) to correlate successfully with Elk Hills oils. Again, the carbon isotopes strongly suggest a Monterey-equivalent source for this oil recovered at 18,015 ft (5491 m).
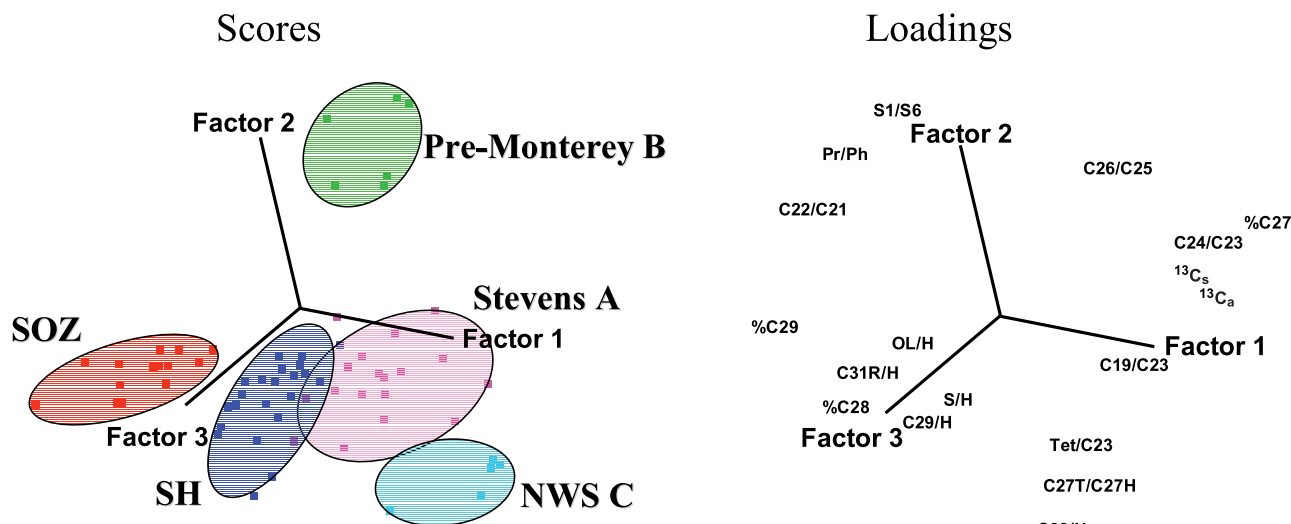
Figure 6. Principal component analysis showing the five Elk Hills oil families (scores) and geochemical variables (loadings) employed. S1/S6 = 13β,17α-diacholestane (20S)/5α-cholestane (20R); Pr/Ph = pristane/phytane from whole crude GC; %C27, %C28, and %C29 = relative percent 5α,14β,17β-cholestane (20S), 5α,14β,17β-ergostane (20S), and 5α,14β,17β-stigmastane (20S) based on m/z 218; C19/C23, C22/C21, C24/C23, and C26/C25 = various tricyclic terpane ratios; Tet/C23 = C24 teteracyclic terpane/C23 tricyclic terpane; C28/H = 17α,18α,21β-28,30-bisnorhopane/17α,21β-hopane; C29/H = 17α,21β-30-norhopane/17α,21β-hopane; OL/H = oleanane/17α,21β-hopane; C31R/H = 17α,21β-30-homohopane (22R)/17α,21b-hopane; C27T/C27H = 17α,18α,21β-25,28,30-trisnorhopane/(18α,21β-22,29,30-trisnorhopane + 17α,21β-22,29,30-trisnorhopane); S/H = sum of 15 steranes/16 hopanes; $^{13}C_s$ and $^{13}C_a$ = stable carbon isotopic composition of the C_{15+} saturate and aromatic hydrocarbons, respectively.

Stable Carbon Isotopes

The Elk Hills C_{15+} saturated and aromatic hydrocarbon fractions ($^{13}C_s$ and $^{13}C_a$, respectively; Table 1) have distinctive heavy isotopic compositions, characteristic of other marine-derived Miocene oils globally. In Figure 7, the Elk Hills oil families plot well to the marine side of the best separating line (marine versus nonmarine-sourced oils; Sofer, 1984), and the SOZ family is clearly distinguished, strongly suggesting a different Monterey source facies.

Based on the whole oil carbon isotope compositions ($^{13}C_{wo}$; Table 1), the less than C_{15+} fraction (% < C_{15} or light-ends) carbon isotopic ratios can be calculated using mass-balance considerations and are given in Table 1 (^{13}C LE). If the light hydrocarbons originated from the Eocene Kreyenhagen Formation, then they would likely have much more negative carbon isotopic compositions, approximately −28 to −29‰, instead of the −23 to −24‰ of the Miocene. In fact, the light hydrocarbons of most of the Elk Hills oils are isotopically more positive than the C_{15+} fractions (heavy-end ^{13}C HE), strongly suggesting that the Monterey generated both the light- and heavy-end components. This is illustrated in Figure 8,

which is a plot of the light-end versus heavy-end carbon isotopic composition. Increasing thermal maturity results in more positive C_{15+} carbon isotope values (Sofer, 1984).

DISCUSSION

Thermal Maturity

The Elk Hills oils represent a wide range of Monterey source rock thermal maturities. Low-maturity indicators are common in the Monterey. Certain key biomarker ratios, in which one of the two related compounds is thermodynamically less stable, represent the maturity ranges of the heavy ends, and the least mature, local sources dominate (local to the reservoir; i.e., see figures 12 and 13 of Reid and McIntyre, 2001). Conversion of Monterey kerogen (1−7 wt.% and about 2−20 vol.% total organic carbon) to fluids involves a volume increase resulting in local overpressure zones, which allows primary oil migration and concentration. At present-day depths of about 5000−7000 ft (1524−2134 m), ongoing, early oil generation from
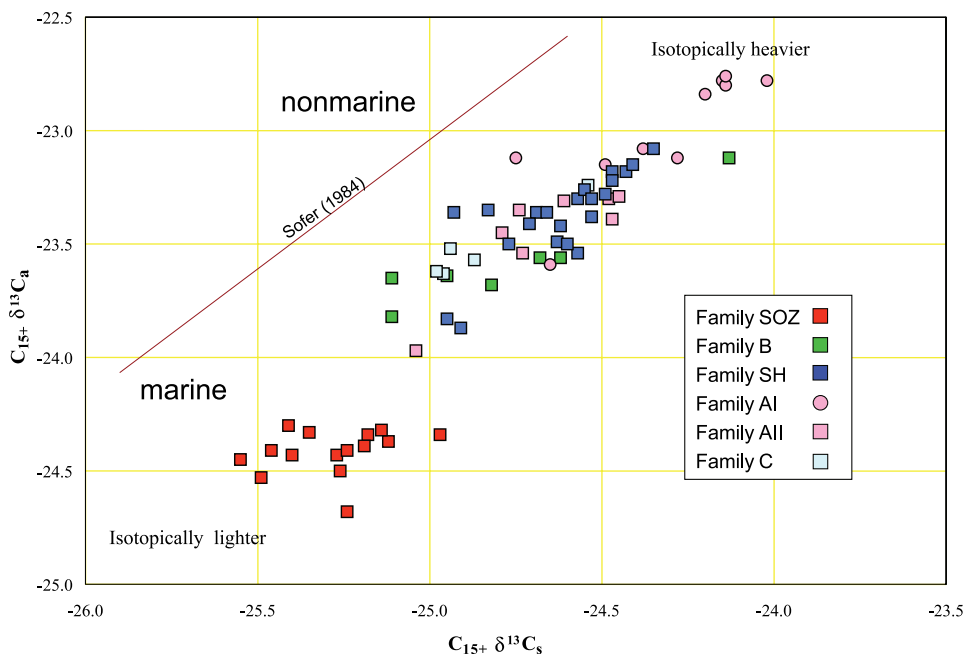
Figure 7. Stable carbon isotope composition of C_{15+} saturated and aromatic hydrocarbons. Shallow oil zone samples (family SOZ) are isotopically distinct, although they are still in the isotopic range of oils generated from the Monterey Formation. Biodegradation generally results in isotopically heavier values (Sofer, 1984).

labile, relatively sulfur-rich kerogen of Monterey source rocks maybe of sufficient magnitude to open micro-fractures, increasing porcelanite permeability. Paleo-depths were likely greater with corresponding higher temperatures.

Figure 9 is a plot of the thermally sensitive terpane biomarkers C_{27} T_s to T_m and a triaromatic sterane ratio (TAS3), with higher ratios suggesting generation from more mature source rocks. The T_s/T_m ratio is

also source dependent, so that maturity differences are valid only for oils in the same family. For example, Kern River Vedder oils are slightly more mature than Elk Hills SOZ samples, but they may or may not be of equivalent maturity to family C. Again, these terpane ratios reflect weighted maturity of the source rocks that generated the heavy ends, with the least mature horizons weighted more because they contain higher absolute concentrations of biomarkers. The triaromatic
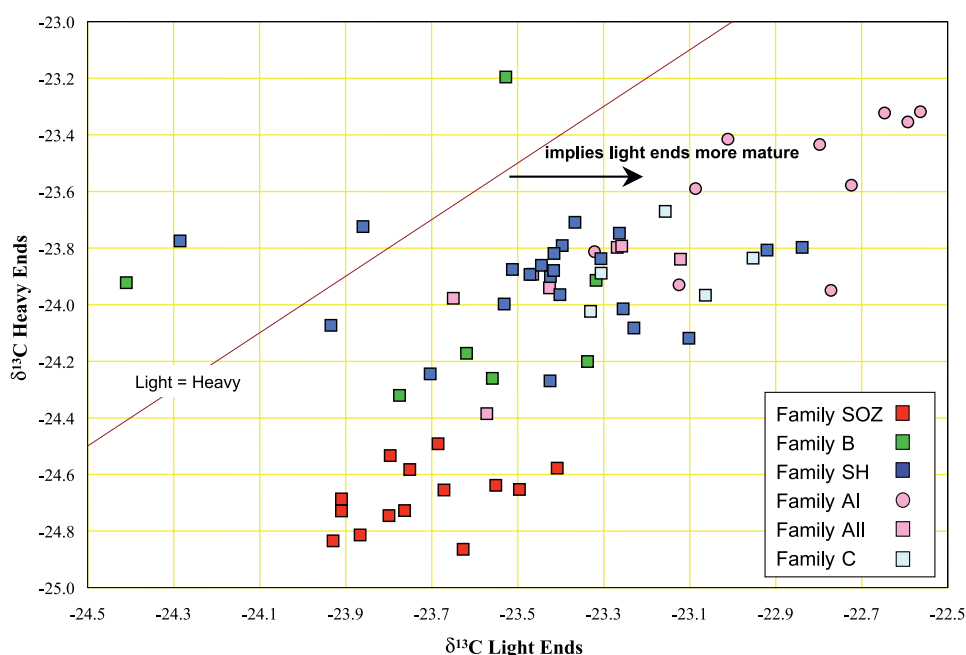

Figure 8. Stable carbon isotope composition of light-end versus heavy-end Elk Hills hydrocarbons. The light-end isotopic values were calculated from the measured heavy ends (C_{15+}) and whole crude isotopic values based on the amount of light ends lost from evaporation ($<C_{15}$; Table 1). The light-end hydrocarbons are isotopically heavier than the heavy ends, suggesting a Monterey source for both the light and heavy ends with the light ends from a more mature Monterey.

Figure 9. Heavy-end biomarker maturity indicators showing thermal-maturity trends in each oil family. Kern River field oils are related to Elk Hills family SOZ oils but appear slightly more mature. C_{27} $T_s/T_m = 18\alpha,21\beta$-22,29,30-trisnorhopane/$17\alpha,21\beta$-22,29,30-trisnorhopane; TAS3 = $[C_{20} + C_{21}]/[\Sigma C_{20} - C_{28}]$ triaromatic steranes (m/z 231).
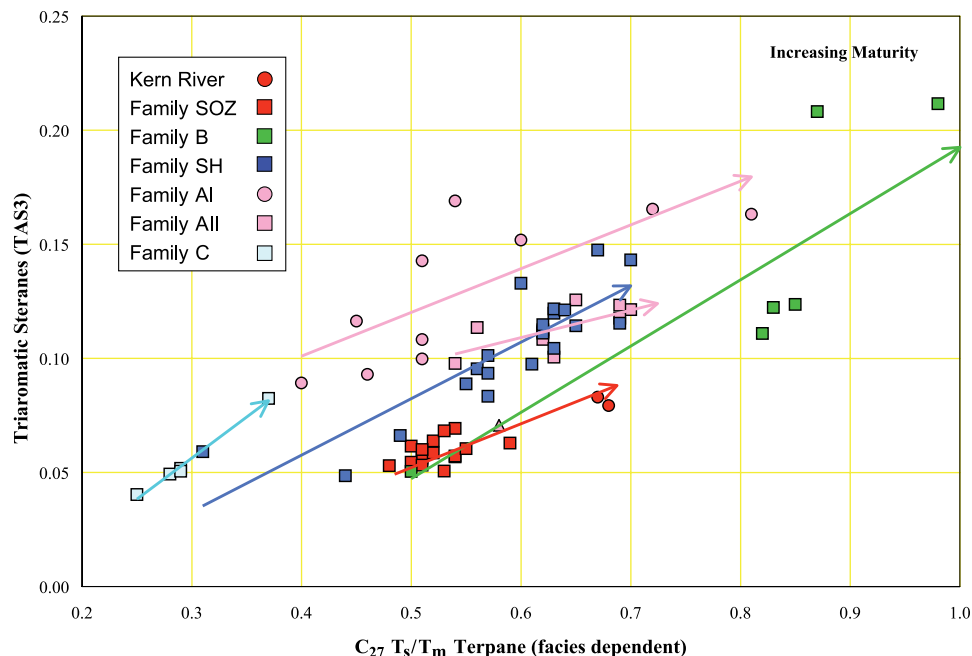

sterane TAS3 ratio ($[C_{20} + C_{21}]/[\Sigma C_{20} - C_{28}]$; $m/z = 231$) appears to be a more universal indicator of maturity, with much less dependence on source. The C_{15+} fraction of SOZ and family C oils both contain the least mature TAS3 ratios.

The range of maturity indicated by family AI samples, which are from the Northwest Stevens and western 29R anticlines, suggests multiple pulses of oil generated from a source rock that is maturing over time.

In contrast, family AII oils, which are mostly from the 31S Stevens turbidite reservoirs, have a more concentrated distribution, suggesting oils are derived from a source rock of consistent maturity.

A graph of the absolute concentrations of two terpane biomarkers (hopane [C_{30}] and bisnorhopane [C_{28}]) relative to the whole crude oil, including light ends, is given in Figure 10. As source rocks mature, fewer heavy-end biomarkers are generated relative to

Figure 10. Absolute biomarker concentrations in whole crude oils: C_{28} bisnorhopane ($17\alpha,18\alpha,21\beta$-28,30-bisnorhopane) versus C_{30} hopane ($17\alpha,21\beta$-hopane). The different trends between families B and C oils versus family A, shales (SH), and SOZ members correspond to different Monterey organic-rich facies. The absolute concentrations of these biomarkers are also a function of thermal maturity.
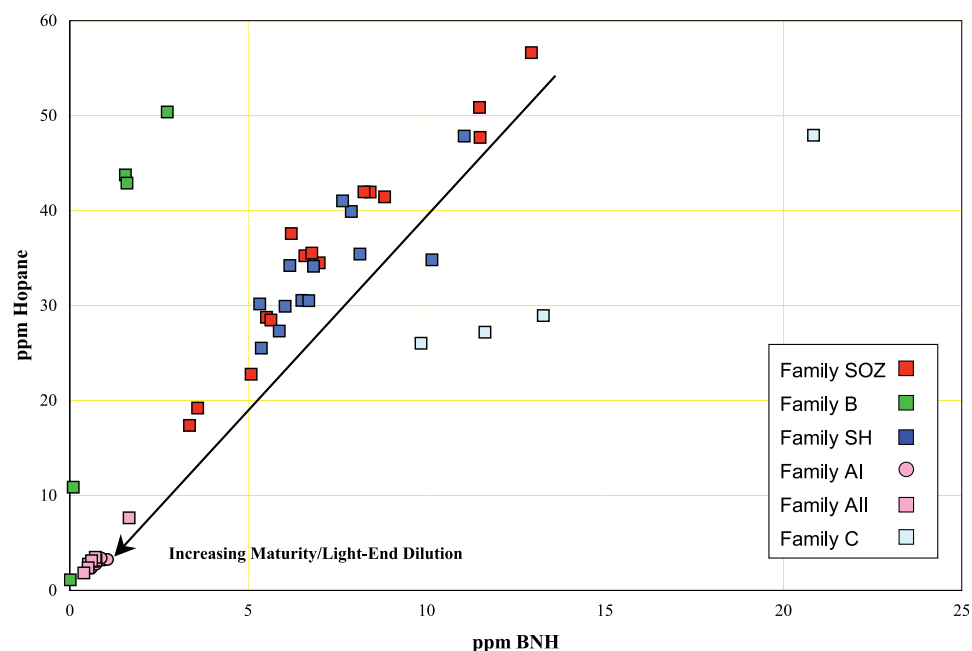
light-end hydrocarbons ($<C_{15}$). If the reservoir or trap is charged and intermixed with local low-maturity oil in addition to oils from various levels of increasing maturity (toward and including subbasin depocenters), then the oil should contain lower absolute concentrations of biomarkers with increasing charge of more mature, downdip generated oil. (Sample CA201, an oil from the upper Main Body B sandstone in well 347-35S, was not included in the figure because it has an anomalous resin content with a low API gravity, inconsistent with the $% < C_{15}$; this sample also appears to have been misclassified and is likely a member of family AII instead of SH.)

Families B and C oils show different trends in Figure 10 because of their abundance of bisnorhopane relative to hopane, both a source and maturity indicator (see Figure 6). The oils from families A, SH, and SOZ all have about the same bisnorhopane/hopane ratio. However, what is probably the most significant aspect of Figure 10 is the low absolute biomarker concentration of family A oils from the Stevens turbidites. Of course, these are, by far, the main oil producers in Elk Hills, and they contain the greatest proportion (or dilution) of more mature light hydrocarbons from the subbasin depocenters by a factor of about 10 or more (3–4 ppm hopane for Stevens turbidite oils versus 30–40+ ppm for the other oil families).

The relationship between the absolute hopane concentrations and the TAS3 maturity ratio for the heavy ends is illustrated in Figure 11. Again, family A oils have constant low amounts of biomarkers, although family AI appears to contain more mature heavy-end components than family AII. In contrast, family SOZ oils have the least mature heavy ends (along with family C) but have a threefold variation in hopane concentration. Much of the biomarker concentration variance in SOZ oils is caused by different degrees of biodegradation, which will be discussed below. In addition, some the SOZ oils may contain water and/or de-emulsifier, which can affect the measurement of $% < C_{15}$ (light ends), resulting in incorrect values for biomarker concentrations.

Families B and SH show maturity trends in the whole crude and heavy ends. Regarding family B, the lower Miocene Carneros oils appear to contain less mature oil than the older Santos samples. Both reservoirs contain Monterey-sourced oil migrating updip, but downsection, probably along faults. For SH oil family samples, an interesting trend is evident in Figure 11, at least for samples from the 29R anticline. The three opal-CT samples contain oil that is clearly less mature

than the oil in the porcelanites that have undergone the opal-CT to quartz transition (four 29R wells). This suggests two pulses of oil charging: an initial wave of oil generated from a less mature source rock into the opal-CT reservoir and a second migration event from a similar but more mature source rock, but occurring after opal-CT porcelanite is converted to quartz phase. The 31S anticline oil in quartz porcelanite reservoirs appears less mature than the 29R anticline oil in corresponding quartz porcelanites. Perhaps the 29R reservoirs received a greater proportion of downdip oil than the 31S reservoirs.

Biodegradation of SOZ Oils

Family SOZ (all of the Reef Ridge and post-Miocene oils in Table 1) comprises a distinctly different type of Monterey oil than that seen in the Stevens turbidites. Because they occur in the youngest reservoirs, they probably originated from the uppermost organic-rich facies of the Monterey (similar to the Monterey facies that generated the Kern River field oil). Many of the SOZ oils have suffered biodegradation because of the low reservoir temperatures. The rate of biodegradation intensifies below reservoir temperatures of about 140°F (60°C). Biodegradation is evident from the whole crude gas chromatograms because the bacteria preferentially consume the n-paraffins, resulting in a lower quality oil (e.g., reduced API gravity and increased sulfur content). The isoprenoids pristane and phytane are more resistant to biodegradation than the n-paraffins (Figure 12), whereas the sterane and terpane biomarkers are the most resistant within the saturated hydrocarbon fraction. Most of the SOZ oils are only mildly degraded, although SOZ oil CA235 is extensively biodegraded (almost no n-paraffins and sterane biomarkers are altered). Other more degraded SOZ oils include CA239, CA230, CA233, and CA234. The API gravities have been significantly lowered in these more extensively degraded oils (Table 1).

However, reservoir temperature is not the only factor relating to the degree of biodegradation. Because oil-degrading bacteria live and reproduce in the aqueous phase, the oil must also be in contact with ground water in order for extensive biodegradation to occur. The most biodegraded SOZ oils occur on the flanks of the 31S anticline, likely corresponding to increased oil-water interaction. Many of the slightly biodegraded SOZ oils have abundant light ends, which is incompatible with biodegradation because bacteria use
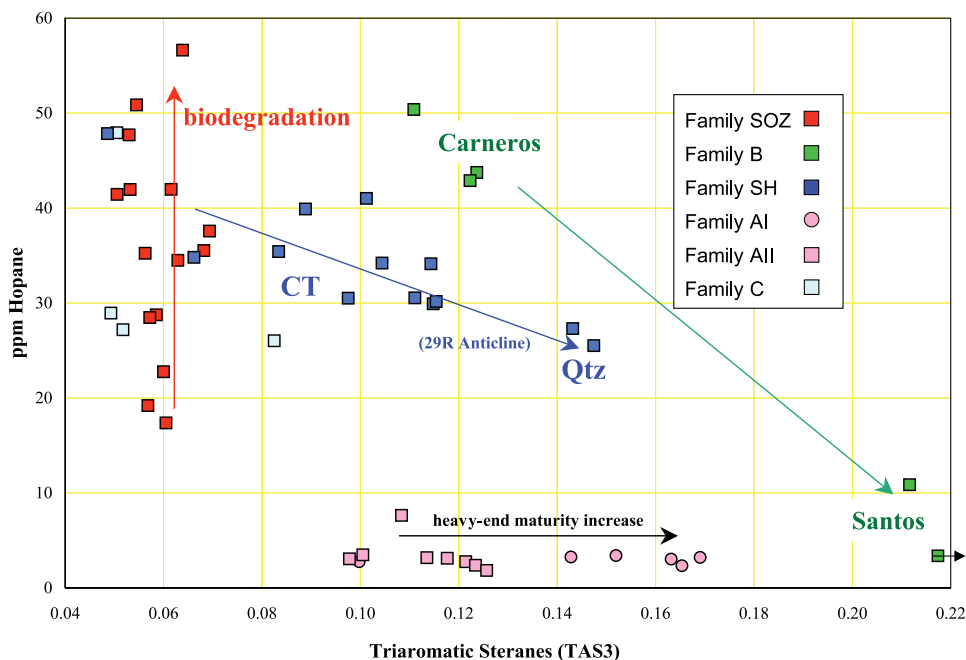
Figure 11. Absolute hopane concentrations versus triaromatic sterane maturity indicator. Family SOZ oils are of equivalent maturity but vary in hopane concentration because of different degrees of biodegradation. The heavy-end components of subfamily AI appear to have originated from more mature source rocks than subfamily AII. The pre-Monterey reservoired oils of family B show an increase in maturity for the older and deeper Santos oils compared to the younger Carneros oils; family B oils were likely generated from the lowermost organic-rich facies of the Monterey. Porcelanite reservoirs in the 29R anticline (western Elk Hills; family Shales) contain more thermally mature oil in the higher temperature microcrystalline quartz phase than in the opal-CT phase reservoirs, perhaps suggesting localized oil generation.

the lighter n-paraffins in preference to C_{15+} n-paraffins. This implies that the SOZ reservoirs have been charged with mature oil, which mixes with the biodegraded initial in-place oil. The quality of these polyhistory oils is determined by the rate of biodegradation versus the rate of recharging.

Figure 12. Pristane to n-C_{17} versus phytane to n-C_{18} plot representing various degrees of family SOZ (shallow oil zone) biodegradation. Bacteria preferentially degrade the n-paraffins relative to the iso-prenoid hydrocarbons. The most degraded oils occur on the flanks of the 31R anticline.
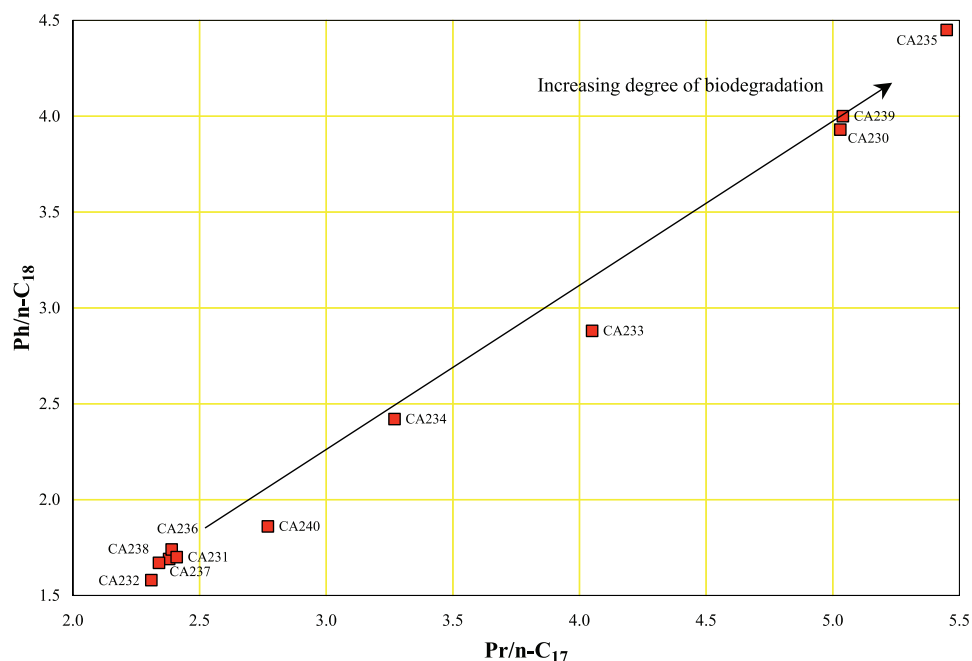
Sequence of Filling Stevens Reservoirs

The geochemical data presented here provide a basis to speculate on the sequence of filling of the Elk Hills reservoirs. On the Northwest Stevens anticline, analysis of the oils (families AI and C) indicates multiple pulses for migration. The initial pulse may have consisted of low-maturity oil derived from the first phase of generation from the Monterey Formation (Figure 13A). Family C oil is restricted to the west end of the anticline and predominantly in a structural-stratigraphic trap. The trap is unique for Stevens reservoirs at Elk Hills in that it was fully formed before all the other traps (Imperato, 1995). The presence of low-maturity oil is consistent with the early trap formation, indicating that this trap had the geometry necessary to accept the initial oil expelled from the Monterey. This oil was generated from the Buttonwillow subbasin, which is structurally adjacent to and downdip of the Northwest Stevens anticline.

The remaining accumulations on the Northwest Stevens anticline contain family AI oils. Although family AI oils have a substantial high-maturity component (Figure 10), these oils have the widest distribution of all Stevens oils on a crossplot of maturity biomarkers (Figure 9). This distribution indicates that oil was derived from a source rock of consistent composition that became increasingly mature. Once the A4–A6 trap formed (probably by middle Pliocene), a continuous stream entered the trap from the Buttonwillow subbasin as the source rock matured and expelled oil (Figure 13B).

The Northwest Stevens anticline and the western 29R structure share some of the same turbidite sand bodies (Figure 4). Sandstone reservoirs on the two structures also share the same oil family (family AI). After filling of the Northwest Stevens anticline reservoirs, oil appears to have spilled into and filled the 24Z trap (Figure 13B). Family AI oil may also have reached the 2B trap on the east nose of the 29R anticline and the 26R reservoir at the west end of the 31S anticline, again moving within turbidite sand bodies from the Northwest Stevens structure.

Oil from Stevens sandstone reservoirs of the 31S anticline belong to family AII. This includes the Main Body B, Western 31S and 26R, and the 2B reservoirs on the eastern nose of the 29R anticline (Figure 13C). The 31S anticline is positioned on a structural high between the Maricopa and Buttonwillow subbasins and is favorably positioned to be charged from either. If family AII oil is derived from both areas, then the source facies must be extremely similar and at the same point of maturity when oil was expelled. Alternatively, only one of the subbasins supplied oil to the 31S sandstone reservoirs and the migration route from the other subbasin was somehow blocked. Maturity biomarkers (Figure 9) show a small maturity band for the AII oils, indicating that the source rock underwent minimal evolution during the period it charged 31S reservoirs. This charge history would be consistent with migration along a newly formed route, such as a developing fault zone on the flanks of the 31S anticline and the quick flooding of the reservoir zones in the late Pliocene or Pleistocene.

The 2B reservoir on the eastern nose of the 29R anticline also contains family AII oil (Figure 13C). The reservoir is a combination structural-stratigraphic trap that has an updip lateral seal formed by the abrupt pinch-out of the 26R sand body. Oil likely migrated from the adjacent 26R reservoir, which is filled to its spillpoint. The 2B reservoir is not filled to its spillpoint, and Reid (1990) speculated that leakage may have occurred through a lower sand body into the updip porcelanite interval. However, family AII oil is not present in the adjacent updip reservoir (as discussed below), indicating that the trap has not leaked and is instead underfilled, possibly because of rerouting of the oil-migration path away from the 31S anticline.

All the Stevens porcelanite reservoirs contain family SH oils (Figure 13D). The distinction between family A and SH oils is remarkable given the close proximity of the reservoir types and clearly indicates a strong segregation of migration routes or histories. A possible explanation is tied to the diagenesis of porcelanite. During migration of family A oils into Stevens sand reservoirs, the adjacent porcelanite intervals may have been at the opal-CT phase of the diagenetic process and had matrix permeabilities too low to permit significant oil to accumulate (Reid and McIntyre, 2001; Schwalbach et al., 2001). Migration into fractures may have occurred, thus accounting for the lower maturity oil present in the opal-CT interval (Figure 9). At some later point, after the sand reservoirs were filled, opal-CT converted to quartz phase and acquired sufficient matrix permeability to become an effective reservoir. Porcelanite reservoirs are the last of the Steven traps to be charged and occurred at a time when the Monterey oil-generating window is the closest to the Elk Hills anticlines. The differences in characteristics between families A and SH oils may reflect compositional variations between distal, basin-floor source rocks that charge the sand reservoir and
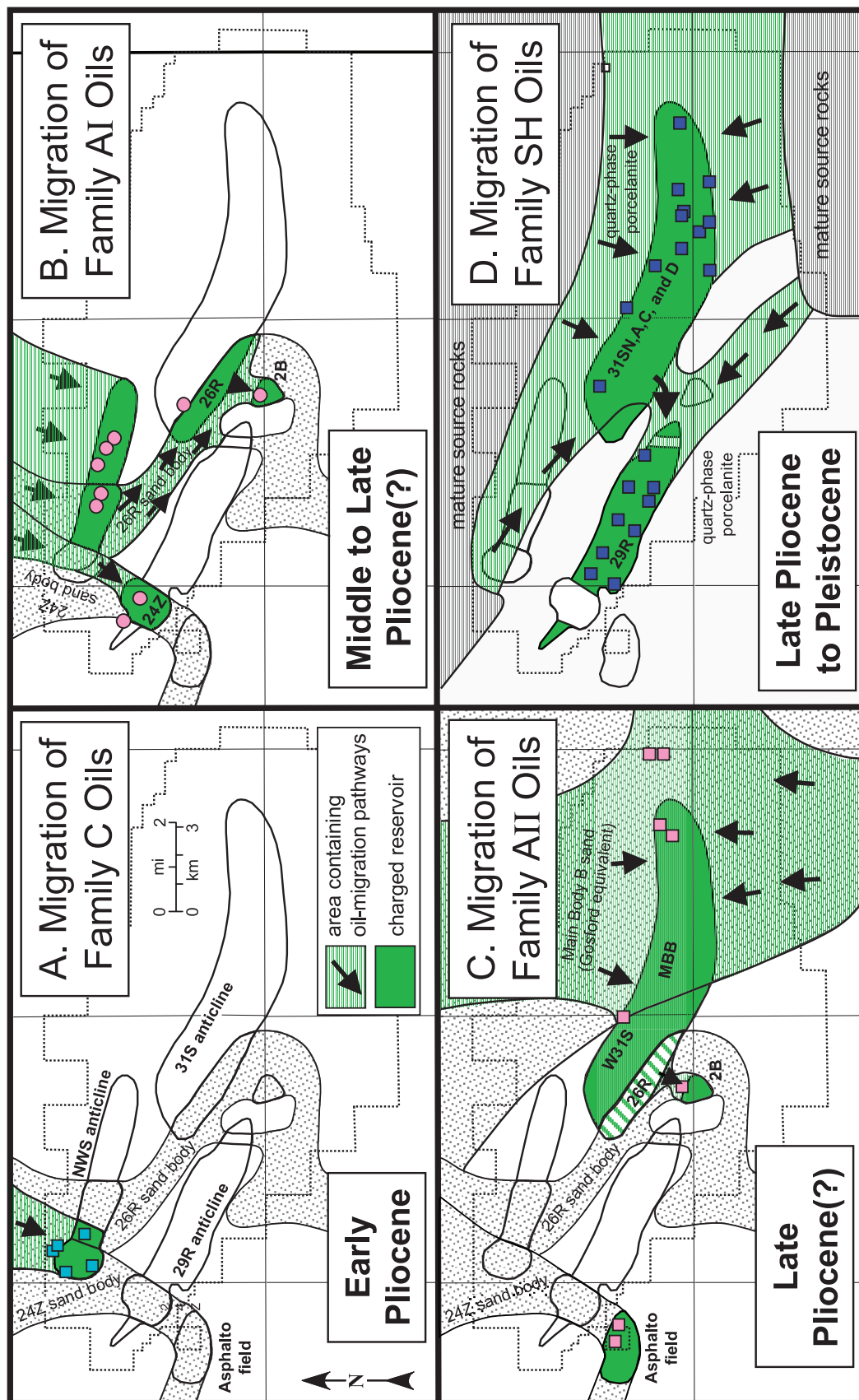
Figure 13. Migration of oil into major Stevens turbidite and porcelanite reservoirs at Elk Hills. (A) Family C oils are restricted to the western end of the Northwest Stevens anticline and are the least mature of the sampled oils. They may have migrated into the earliest formed traps in the Northwest Stevens anticline along turbidite sand bodies updip from the Buttonwillow subbasin. (B) Oils of family AI are likely derived from the Buttonwillow subbasin and filled reservoirs in the central and eastern Northwest Stevens anticline. Oil spilled from the Northwest Stevens traps and followed turbidite sand bodies updip into the 26R, 2B, and 24Z reservoirs. (C) Family AII oils probably are from both the Buttonwillow and Maricopa subbasins and migrated into the 31S reservoirs following the Main Body B submarine-fan complex. Oil possibly leaked into the 26R sand body and spilled into the 2B trap. The occurrence of family AII oil in the Asphalto field remains a dilemma. (D) Family SH oils occur in porcelanite reservoirs across the entire field and are sandwiched stratigraphically between families AI and AII reservoirs. Migration likely occurred after filling of the turbidite reservoirs and after development of more favorable porosity because of transition of porcelanite from opal-CT to quartz phase.

more proximal (lower slope?) areas where organic material was deposited on the flanks of actively growing structures.

The presence of family AII oil in the Asphalto field west of Elk Hills presents a migration dilemma because obvious migration routes are not supported by the geochemical data. Low-permeability opal-CT phase porcelanite on the 29R anticline should have blocked oil migration from the 2B area into 24Z or Asphalto. The other option of migration from the 24Z and Northwest Stevens anticline reservoirs seems unlikely because of the absence of family AII samples on this trend. This problem demonstrates that the distinction between family AI and AII is very subtle, and there may be limits to the extent oil families should be used to interpret migration history.

CONCLUSIONS

Five principal oil families, all generated from different organofacies of the Monterey, were determined to exist at Elk Hills based on multivariate statistical analyses of genetically important biomarker distributions and bulk carbon isotope compositions. Family C oil at the west end of the Northwest Stevens anticline contains the least mature oil and was the first to migrate into the Elk Hills areas. The remaining Stevens sandstone reservoirs have family A oil. These oils contain the most light-end hydrocarbons and were likely generated from organic-rich facies of the Monterey, stratigraphically adjacent to the turbidite sand bodies in location on or near the basin floor. Family SH oils, in porcelanite reservoirs, are widespread across the entire field and were derived from similar, albeit more local Monterey facies interbedded with quartz porcelanite. The pre-Monterey oils of family B appear to have been generated from lowermost, organic-rich Monterey facies. These have different biomarker distributions and are the most thermally mature, but also have the distinct isotopic signature of the Monterey. Family SOZ oils are commonly biodegraded, occur in shallow post-Monterey reservoirs, and were probably generated from uppermost organic-rich Monterey facies.

The aerial distribution of Stevens oil families (Figure 13) represents the development of source areas and oil-migration routes. Entrapment of the Monterey's initially generated and expelled low-maturity oil is very limited because migration routes to Elk Hills were not established and few traps had formed. By the time most of the Stevens structures form, the source areas located on or near the basin floors are generating high-maturity oil and expelling into the Stevens sand bodies. Migration routes may have altered over time, especially on the 31S anticline, where family AII oil was possibly diverted after charging the 31S reservoirs. Through the late Pliocene and Pleistocene, the thermally mature areas of the Buttonwillow and Maricopa subbasins expanded and approached the flanks of the Elk Hills anticlines. By the time quartz-phase porcelanite reservoirs developed sufficient permeability to accumulate oil, areas downdip on the anticlinal limbs were mature and expelling high-maturity oil.

The results of the carbon isotopic analyses suggest that both the heavy- and light-end components of Elk Hills reservoirs originated from the Monterey (no Eocene Kreyenhagen component). Oil was generated at various thermal-maturity stages (at different times and different depths in the subbasins) and mixed in the reservoir. Family A oils, from Stevens turbidites, by far the main oil producers at Elk Hills, contain a factor of 10 or more of the mature light hydrocarbons from the subbasin depocenters than the other families.

One conspicuous dichotomy noticed early in interpreting the chemistry of the Elk Hills Monterey oils was that the biomarkers indicate a low thermal maturity for the source, almost immature. However, the API gravities of most Elk Hills oils are between 30 and 40° with 40–50% light ends. These abundant lighter hydrocarbons and relatively high gravities indicate at least moderate thermal maturity for the source. Most biomarkers occur in the heavy C_{15+} fraction and are concentrated in low-maturity, early-generated oil. Subsequent oil expelled from deeper, more thermally mature source horizons contains more mature biomarker distributions, but at much lower absolute concentrations. Most of the Elk Hills oils produced from the Stevens sandstones appear to be the result of mixing, with small quantities of biomarker-rich low-maturity Monterey oil (migrating through the reservoirs prior to trap formation) being progressively diluted by increasingly mature oil from downdip source rocks containing abundant light ends. The question as to the source of these mature, light-end hydrocarbons, both in the Stevens and pre-Monterey reservoirs, has been answered based on carbon isotope compositions; the Monterey also generated the light-end hydrocarbons instead of the older Eocene Kreyenhagen.

What is remarkable about the Elk Hills oil families is the strong correlation with the reservoir interval (Table 1; Figure 2). The different oil families, generated from stratigraphic and geographic variations in the Monterey organic-rich facies, correspond to reservoir horizons. This suggests minimal upsection, cross-stratigraphic migration from the basin depocenters to Elk Hills; specific inter-Monterey source-reservoir packages extend downdip into the basin with good intervening seals. However, the pre-Monterey reservoired oils (family B) in the Carneros and Santos formations also contain Monterey oils, albeit at higher thermal maturities. It appears that the older Monterey source horizons can charge even older reservoir units as updip, but downsection migration occurs.

The Pliocene SOZ oils, which are isotopically distinct from other Elk Hills oils, have been biodegraded to different degrees. The most biodegraded oils have the lowest API gravities and occur on the flanks of the 31S anticline. Although slightly more positive (not caused by biodegradation), the carbon isotopic composition of SOZ oils suggests yet another Monterey source facies (perhaps the youngest) with charging of Pliocene reservoirs. The SOZ oils are not simply the result of vertical leakage in the Elk Hills area from any of the older Miocene reservoirs.

REFERENCES CITED

Bandy, O. L., and R. E. Arnal, 1969, Middle Tertiary basin development, San Joaquin Valley, California: Geological Society of American Bulletin, v. 80, p. 783–819.

Bartow, J. A., 1991, The Cenozoic evolution of the San Joaquin Valley, California: U.S. Geological Survey Professional Paper 1501, 40 p.

California Division of Oil, Gas, and Geothermal Resources, 2003, 2002 annual report of the state oil and gas supervisor: Sacramento, California, California Department of Conservation Publication No. PR06, 263 p.

Church, H. V., and K. Krammes, 1957, Correlation section no. 9 across central San Joaquin Valley from San Andreas fault to Sierra Nevada foothills, California: Pacific Section, AAPG Geologic Names and Correlations Committee.

Dunwoody, J. A., 1986, Correlation section no. 8 (revised) across southern San Joaquin Valley from San Andreas fault to Sierra Nevada foothills: Pacific Section, AAPG Geologic Names and Correlations Committee.

Fiore, P. E., D. D. Pollard, B. R. Currin, and D. D. Miner, 2004, Tectonic history and evolution of the faulting at Elk Hills oil field: A mechanical study (abs.): Pacific Section, AAPG, Annual Convention Abstract, www.searchanddiscovery.com /documents/abstracts/2004pacific/index.htm.

Graham, S. A., 1978, Role of Salinian block in evolution of San Andreas fault system, California: AAPG Bulletin, v. 62, p. 2214–2231.

Graham, S. A., and L. A. Williams, 1985, Tectonic, depositional, and diagenetic history of Monterey Formation (Miocene), central San Joaquin basin, California: AAPG Bulletin, v. 69, p. 365–411.

Graham, S. A., R. G. Stanley, J. V. Bent, and J. B. Carter, 1989, Oligocene and Miocene paleogeography of central California and displacement along the San Andreas fault: Geological Society of America Bulletin, v. 101, p. 711–730.

Harding, T. P., 1976, Tectonic significance and hydrocarbon trapping consequences of sequential folding synchronous with San Andreas faulting, California: AAPG Bulletin, v. 60, p. 356–378.

Imperato, D. P., 1995, Studies of the stratigraphy and structure of the Great Valley of California and implications for plate tectonics: Ph.D. dissertation, University of California at Santa Barbara, Santa Barbara, California, 271 p.

Isaacs, C. M., 1981, Field characterization of rocks in the Monterey Formation along the coast near Santa Barbara, California, in C. M. Isaacs, ed., Guide to the Monterey Formation in the California coastal area, Ventura to San Luis Obispo: Pacific Section, AAPG Field Trip Guidebook, v. 52, p. 39–53.

Isaacs, C. M., and J. Rullkötter, 2001, eds., Cooperative Monterey organic geochemistry study, the Monterey Formation: From rocks to molecules: New York, Columbia University Press, 608 p.

Kaplan, I. R., 2000, ed., Collection of papers about the oil, gas, and source rock investigations carried out in the San Joaquin, Santa Maria, Santa Barbara, Ventura and Los Angeles basins, California: Pacific Section AAPG, CD-ROM Series 1.

Kruge, M. A., 1986, Biomarker geochemistry of the Miocene Monterey Formation, west San Joaquin basin, California: Implications for petroleum generation: Organic Geochemistry, v. 10, p. 517–530.

MacPherson, B. A., 1978, Sedimentation and trapping mechanism in upper Miocene Stevens and older turbidite fans of southeastern San Joaquin Valley, California: AAPG Bulletin, v. 62, p. 2243–2278.

Nilsen, T. H., 1987, Paleogene tectonics and sedimentation of coastal California, in R. V. Ingersoll and W. G. Ernst, eds., Cenozoic basin development of coastal California, Rubey volume 6: Englewood Cliffs, New Jersey, Prentice-Hall, p. 81–123.

Peters, K. E., T. D. Elam, M. H. Pytte, and P. Sundararaman, 1994, Identification of petroleum systems adjacent to the San Andreas fault, California, U.S.A., in L. B. Magoon and W. G. Dow, eds., The petroleum system—From source to trap: AAPG Memoir 60, p. 423–436.

Peters, K. E., C. C. Walters, and J. M. Moldowan, 2005, The biomarker guide: Cambridge, United Kingdom, Cambridge University Press, 1024 p.

Reid, S. A., 1990, Trapping characteristics of upper Miocene turbidite deposits, Elk Hills field, Kern County, California, in J. G. Kuespert and S. A. Reid, eds., Structure, stratigraphy and hydrocarbon occurrences of the San Joaquin basin, California: Pacific Section, AAPG, guidebook GB65, p. 141–156.

Reid, S. A., 1995, Miocene and Pliocene depositional systems of the southern San Joaquin basin and formation of sandstone reservoirs in the Elk Hills area, California, in A. E. Fritsche, ed., Cenozoic paleogeography of the western United States—II: Pacific Section, SEPM, book 75, p. 131–150.

Reid, S. A., and J. L. McIntyre, 2001, Monterey Formation porcelanite reservoirs of the Elk Hills field, Kern County, California: AAPG Bulletin, v. 85, p. 169–189.

Schwalbach, J. R., W. C. Benmore, S. A. Reid, R. D. Tucker, and E. J. Hanley, 2001, Silica phase and compositional controls

on pore throat distributions— Porcelanite and siliceous shale of the Elk Hills field, California (abs.): AAPG Annual Meeting Program, v. 10, p. A181.

Sofer, Z., 1980, Preparation of carbon dioxide for stable carbon isotope analysis of petroleum fractions: Analytical Chemistry, v. 52, p. 1389–1391.

Sofer, Z., 1984, Stable carbon isotope compositions of crude oils: Application to source depositional environments and petroleum alteration: AAPG Bulletin, v. 68, p. 31–49.

Villanueva, L., and J. Kappeler, 1989, Correlation section 27 through central San Joaquin Valley from Turk anticline (Cantua Creek) to the Transverse Range: Pacific Section, AAPG Geologic Names and Correlations Committee.

Webb, G. W., 1981, Stevens and earlier Miocene turbidite sandstone, southern San Joaquin Valley, California: AAPG Bulletin, v. 65, p. 438–465.

West, N., R. Alexander, and R. I. Kagi, 1990, The use of silicalite for rapid isolation of branched and cyclic alkane fractions of petroleum: Organic Geochemistry, v. 15, p. 499–501.

Zieglar, D. L., and J. H. Spotts, 1978, Reservoir and source-bed history of Great Valley, California: AAPG Bulletin, v. 62, p. 813–826.